

Sum Rate Characterization of Joint Multiple Cell-Site Processing *

Oren Somekh Benjamin M. Zaidel Shlomo Shamai (Shitz)

August 17, 2005

Abstract

The sum-rate capacity of a cellular system model is analyzed, considering the uplink and downlink channels, while addressing both non-fading and flat-fading channels. The focus is on a simple Wyner-like multi-cell model, where the system cells are arranged on a circle, assuming the cell-sites are located at the boundaries of the cells. For the uplink channel, analytical expressions of the sum-rate capacities are derived for intra-cell TDMA scheduling, and a “Wide-Band” (WB) scheme (where all users are active simultaneously utilizing all bandwidth for coding). Assuming *individual per-cell power constraints*, and using the Lagrangian uplink-downlink duality principle, an analytical expression for the sum-rate capacity of the downlink channel is derived for non-fading channels, and shown to coincide with the corresponding uplink result. Introducing flat-fading, lower and upper bounds on the average per-cell sum-rate capacity are derived. The bounds exhibit an $O(\log_e K)$ multi-user diversity factor for a number of users per-cell $K \gg 1$, in addition to the array diversity gain. Joint multi-cell processing is shown to eliminate out-of-cell interference, which is traditionally considered to be a limiting factor in high-rate reliable communications.

*This paper was presented in part at the 9th Canadian Workshop on Information Theory (CWIT), Montréal, Québec, June 2005, and at the 3rd International Workshop on Signal Processing for Wireless Communications (SPWC 2005), London, Great Britain, June 2005. The authors are with the department of Electrical Engineering, Technion - IIT, Haifa 32000, Israel. E-mails: orens@tx.technion.ac.il, benny@inter.net.il, sshlomo@ee.technion.ac.il.

1 Introduction

The growing demand for ubiquitous access to high-data rate services, has spurred intensive research, analyzing the performance of various wireless communications systems. Cellular systems are of major interest as the most common approach for providing continuous services to mobile users, in both indoor and outdoor environments. In particular, efforts are made to identify efficient systems which guarantee enhanced performance.

In general, exploring the possible methods for enhancing system performance, *joint processing* of signals related to different users is evidently the most appealing approach in either the uplink or downlink channels. Due to complexity and inherent system considerations, *single-user detection* at the mobile receivers is the common practice for the downlink channel, yielding a Gaussian noise plus interference channel model. The less restrictive complexity constraints at the cell-site advocate the use of *transmitter based joint preprocessing* for system performance enhancement (see [1] for a downlink capacity analysis where no transmitter (cell-sites) cooperation is assumed, and multiuser detection is employed at the mobile receivers for mitigating co-channel interference). The *uplink* channel is a *multiple access* channel (MAC), and *joint processing of the received signals* at the cell-sites is the appropriate approach (reasonably assuming no user cooperation, though multiuser cooperation has been considered recently [2]). The *downlink* channel is a *broadcast* channel (BC). The MAC-BC duality principle in different frameworks [3] – [6] provides the firm information theoretic connections between these seemingly different models, and shall be used as a key tool in the following.

Starting with the uplink channel, an attractive analytically tractable model for a multi-cell system is suggested by Wyner in [7]. Accordingly, the system's cells are ordered in either an infinite linear array, or in the familiar two-dimensional hexagonal pattern (also infinite). It is assumed that only adjacent-cell interference is present and characterized by a single parameter, a scaling factor $\alpha \in [0, 1]$. Considering non-fading channels and a “wideband” transmission scheme, where all bandwidth is available for coding (as opposed to *random* spreading), the throughputs obtained with optimum and linear MMSE *joint* processing of the received signals from *all* cell-sites are derived (see also [8] for an earlier relevant work). These results are extended to flat-fading channels in [9], where it is observed that fading may increase the throughput under certain conditions.

In contrast to the centralized processing approach of [7] and [9], the Wyner model was also recently used in [10] [11] to demonstrate the efficiency and near-optimal performance of distributed cell-sites processing algorithms, achieved by local message passing among adjacent cell-sites.

Single-cell-site processing in a multi-cell environment is considered in [12]. Adhering again to the Wyner model, and the wideband transmission scheme, the users are divided into intra-cell vs. other-cell users, with respect to which different knowledge at the receiver regarding the structure of the transmissions may be assumed. The receiver processes only the signals received at the local cell-site, and it is ignorant of the codebooks employed by users of other cells, interpreting their interference as Gaussian noise (the results are extended to joint two-cell-site processing in Part II of the paper).

Randomly-spread DS-CDMA systems have also been considered in many information theoretic analyses, in view of their widespread practical use. Important results for random spreading were obtained in [13] and [14], while focusing on *a single isolated cell*. The asymptotic setup is considered, in which both the number of users and the processing gain go to infinity, while their ratio goes to some finite constant (referred to as the “cell load”). Using results from the theory of random matrices [15], limiting analytical *deterministic* expressions for the spectral efficiency of linear and the optimum multiuser receivers are derived, for both non-fading [13] and flat-fading channels [14]. The results are extended to the Wyner [7] *linear* cell-array multi-cell model with *single-cell-site* processing in [16], for non-fading channels, and in [17] for flat-fading channels, demonstrating the impact of undecodable out-of-cell interference in this setting (see [18] for a straightforward extension of the results to the case in which out-of-cell interference extends to more than just the two adjacent cells). The capacity under outage constraint for “strongest-user-only” receivers is derived in [19], for a setting in which the users employ equal rates and transmit powers, and the receiver decodes the transmissions of the largest subset of intra-cell users that can be reliably decoded (see also [20] for the corresponding analysis in a single-cell setting, and [21] for a related analysis). The spectral efficiency with *both* joint-multiple-cell-site processing and random spreading was recently derived in [22], demonstrating the dramatic enhancement of spectral efficiency due to joint processing.

Turning to the downlink channel, a particular attention has been given to the case in which both transmitter and receivers have full channel state information. In a pioneer-

ing work [23], a set of achievable rates for the multi-input multi-output (MIMO) BC was obtained by applying Costa’s “dirty paper” coding (DPC) principle [24], effectively eliminating the impact of additive uncorrelated interference while fully known (non-causally) at the transmitter, but not at the receiver. A novel transmission scheme based on the idea of “ranked known interference” is employed, according to which the transmitter decomposes the channel into an ordered (or ranked) set of interference channels, for which the “dirty paper” coding principle can be applied. The above scheme was first adopted for a multi-cell system in [25], while focusing on Wyner’s [7] infinite linear cell-array model. Here, a simple LQ -factorization based linear pre-processing scheme, combined with “dirty paper” coding is analyzed, and the attainable average rates, for an *overall* system power constraint, are shown to approach those of optimum joint processing at the high signal-to-noise ratio (SNR) region.

In [26], the problem of transmitter optimization to maximize the downlink sum-rate of a *multiple antenna* cellular system is addressed, but with a more realistic *separate* power constraint per each cell-site. To perform the resulting non-convex optimization the duality between the BC and the MAC is used. A related result is obtained in [3], where a connection between the MAC-BC (uplink-downlink) duality and the Lagrangian duality in minimax optimization is established. This connection allows the BC-MAC duality to be generalized to BCs with arbitrary linear constraints.

The BC-MAC duality was first reported in [4] and [5]. This observation was extended in [5], and [6] to include a generalized MIMO system model. It is worth mentioning that the MIMO Gaussian BC is in general a non-degraded BC, and it was only recently shown [27] that its capacity region coincides with the “dirty paper” capacity region [23]. Analyses with no inter-cell cooperation and/or dirty-paper coding on the downlink are standard, see [28], [29], comparisons in [30], and references therein.

The “dirty paper” principle is also used in [30] [31], where the problem of providing the best possible service to new users joining the system without affecting existing users is addressed. The new users are required to be invisible, interference-wise, to existing users, and the network is referred to as “PhantomNet”. In this framework setups including multiple users, multiple antennas, and multiple cells, on both the uplink and the downlink channels, can be addressed. In [32], another generic framework is proposed for the study of base station cooperation in the downlink, to overcome the co-channel interference lim-

ited nature of conventional non-cooperative cellular systems. Numerical analyses of a joint transmission scheme (utilizing DPC), and a cooperative base station selection procedure, are performed, demonstrating the advantage of base station cooperation, while assuming a “realistic” fading channel model. Throughput outage calculations of several cooperative joint transmission schemes, including “zero-forcing” and DPC, are reported in [33]. The numerical results demonstrate the value of employing coherent downlink base station coordination.

In this paper a novel “Wyner-like” simple cellular (multi-cell) system model is introduced, and the average per-cell sum-rate capacity with joint multiple cell-site processing in both uplink and downlink channels is analyzed, while addressing both non-fading and flat-fading channels. It is assumed that the system cells are arranged on a *circle*, as depicted in Fig. 1. Furthermore, it is assumed that the cell-sites are located at the *boundaries* of the cells, and that the signals transmitted by each of the users is received in the uplink channel only by the two cell-sites at the edges of its cell. Analogously, in the downlink channel, each user receives only the signals transmitted by the two cell-sites at its cell edges. This system model focuses on users operating at the cell boundaries, and models a practical soft handoff scenario involving the two nearest cell-sites. The choice of a circular array setting is motivated by its symmetry properties, that make it more amenable to analytical analysis. Note that, as reviewed above, previous works on multiple-cell systems often considered a *linear* cell-array setting, e.g. see [7], [12], [9], [25], [16], [22]. However, the linear and circular models are expected to be equivalent in the large number of cells limit, as shown for example in the setting of [22] (see also [34]). In addition, the underlying model in the above analyses, i.e., the Wyner model of [7], focuses on users operating at the *centers* of each of the cells, with each user being either received by *three* cell-sites, in the uplink channel, or receiving, in the downlink channel, the signals of three cell-sites (the local cell-site and the two cell-sites of adjacent cells).

In the analysis to follow the uplink channel with equal transmit powers is considered first. Assuming full channel state information (CSI) is available to the joint multiple-cell site processor (but not to the transmitting users), the focus is on intra-cell *time-division multiple-access* (TDMA) scheduling (i.e., a single active user per-cell), and on the “wideband” (WB) transmission scheme mentioned above, according to which all users simultaneously occupy the available bandwidth, and all bandwidth may be utilized for

coding (no random spreading employed, see [7], [12], [9]). For non-fading channels an analytical expression for the average per-cell sum-rate capacity is derived, using well known results on the eigenvalues of circulant matrices [34]. It is shown that both TDMA and the WB scheme are equivalent in this setting, as also reported in [7]. Introducing flat fading, an analytical result for the average per-cell sum-rate capacity with TDMA scheduling is derived using a relatively recent result by Narula [35], originally obtained for a time-varying two taps inter-symbol interference (ISI) channel. For the WB scheme, the limiting setup as the number of users per cell grows to infinity (while fixing the total intra-cell transmit power) is considered, and the limiting average per-cell sum-rate capacity is derived by exploiting again the circular structure of the channel transfer matrix. The limiting WB scheme is shown to exhibit the full diversity scale of the system, and the corresponding sum-rate result constitutes an upper bound for the sum-rate capacity with any finite number of users per cell (and in particular with the TDMA scheme), as shown in [9].

The downlink channel is considered next, while assuming full CSI is available to the joint multiple cell-site transmitter, and that own CSI is available to the users' receivers. Here, individual per cell-site power constraints are invoked. The sum-rate capacity expression as formulated in [3], using the uplink-downlink (MAC-BC) duality principle, is employed as the main tool for the derivations. Considering the dual uplink (MAC) channel, an exact expression for the downlink average per-cell sum-rate capacity is derived for non-fading channels, and shown to be identical to the corresponding uplink result. For Rayleigh flat fading channels, upper and lower (achievable rate) bounds are derived, while focusing on the asymptotic setup in terms of the number of users per cell. Both bounds exhibit an $O(\log_e K)$ multiuser diversity factor, where K denotes the number of users per cell, in addition to the inherent array diversity gain. This comes in contrast to the corresponding results for the uplink channel while employing the WB scheme, for which, at best, the array diversity gain of 2 can be obtained. The uplink-downlink duality principle guarantees however the same uplink multiuser diversity features with *proper* scheduling and availability of CSI, as also demonstrated here. For both uplink and downlink channels, joint multi-cell processing eliminates out-of-cell interference, which is traditionally considered to be a limiting factor in high-rate reliable communications.

To complete the analysis, the average per-cell spectral efficiency (bits/sec/Hz) for both uplink and downlink channels is also considered, and particular attention is given to the

extreme-SNR characterization of the results [36], [14]. System performance measures of interest such as the minimum transmit E_b/N_0 that enables reliable communication, and the extreme-SNR slopes are derived, and provide a deeper insight into the nature of the results obtained for the various settings addressed here. The rest of this paper is organized as follows. Section 2 is devoted to the analysis of the uplink channel, while Section 3 presents the corresponding analysis of the downlink channel. Finally, Section 4 ends the paper with a summary and some concluding remarks.

2 Uplink Sum-Rate Capacity

2.1 Uplink System Model

Consider a circular array of M cells with K users per cell. The vector baseband representation of the signals received at the system's cell-sites is given for an arbitrary time index by

$$\mathbf{y}_{ul} = \mathbf{H}_M \mathbf{x}_{ul} + \mathbf{z}_{ul} . \quad (2-1)$$

The $M \times KM$ channel transfer matrix \mathbf{H}_M is

$$\mathbf{H}_M = \begin{pmatrix} \mathbf{a}_0 & \mathbf{0} & \cdots & \mathbf{0} & \mathbf{b}_0 \\ \mathbf{b}_1 & \mathbf{a}_1 & \mathbf{0} & \cdots & \mathbf{0} \\ \mathbf{0} & \mathbf{b}_2 & \mathbf{a}_2 & \ddots & \vdots \\ \vdots & \ddots & \ddots & \ddots & \mathbf{0} \\ \mathbf{0} & \cdots & \mathbf{0} & \mathbf{b}_{M-1} & \mathbf{a}_{M-1} \end{pmatrix} , \quad (2-2)$$

where \mathbf{a}_m and \mathbf{b}_m are $1 \times K$ row vectors denoting the channel complex fading coefficients, experienced by the K users of the m th and $[(m - 1) \bmod M]$ th cells, respectively, when received by the m th cell-site. It is also assumed that the fading processes are i.i.d. among different users, and can be viewed for each user as an ergodic process with respect to the time index.

Channel state information (CSI) is assumed to be available to the joint multiple-cell-site receiver only, whereas the users cannot cooperate their transmissions in any way. Gaussian codebooks therefore conform with the capacity achieving statistics, and the symbols trans-

mitted by each of the users, $\{\mathbf{x}_{ul}\}_i^{MK}$, are taken as i.i.d. zero-mean circularly symmetric Gaussian random variables, with variance P , representing the *equal* average transmit power of each of the users. \mathbf{z}_{ul} represents the zero mean circularly symmetric AWGN vector, and it is assumed that $E\{\mathbf{z}_{ul}\mathbf{z}_{ul}^\dagger\} = \mathbf{I}_M$, where \mathbf{I}_M is the $M \times M$ identity matrix (P is thus equal to the transmit SNR of the users).

2.2 Preliminaries

The ergodic average per-cell sum-rate capacity of the uplink channel is given by

$$C_{\text{ul}} = \frac{1}{M} E_{H_M} \left\{ \log \left(\mathbf{I}_M + \frac{\bar{P}}{K} \mathbf{H}_M \mathbf{H}_M^\dagger \right) \right\}, \quad (2-3)$$

where $\bar{P} \triangleq KP$ is the total intra-cell transmit power, and the expectation is taken with respect to the fading coefficients (unless explicitly specified, all $\log(\cdot)$ expressions may be taken with an arbitrary basis). The matrix $\mathbf{H}_M \mathbf{H}_M^\dagger$ in (2-3) is an $M \times M$ matrix given by

$$\left[\mathbf{H}_M \mathbf{H}_M^\dagger \right]_{m,n} = \begin{cases} \mathbf{a}_m \mathbf{a}_m^\dagger + \mathbf{b}_m \mathbf{b}_m^\dagger & n = m \\ \mathbf{b}_m \mathbf{a}_{\widehat{m-1}}^\dagger & n = \widehat{m-1} \\ \mathbf{a}_m \mathbf{b}_{\widehat{m+1}}^\dagger & n = \widehat{m+1} \\ 0 & \text{otherwise} \end{cases} \quad (2-4)$$

$$m = 0, 1, \dots, (M-1),$$

where

$$\widehat{m+1} \triangleq (m+1) \bmod M \quad ; \quad \widehat{m-1} \triangleq (m-1) \bmod M. \quad (2-5)$$

For example, in the particular case of $M = 4$, $\mathbf{H}_M \mathbf{H}_M^\dagger$ boils down to

$$\mathbf{H}_4 \mathbf{H}_4^\dagger = \begin{pmatrix} \mathbf{a}_0 \mathbf{a}_0^\dagger + \mathbf{b}_0 \mathbf{b}_0^\dagger & \mathbf{a}_0 \mathbf{b}_1^\dagger & 0 & \mathbf{b}_0 \mathbf{a}_3^\dagger \\ \mathbf{b}_1 \mathbf{a}_0^\dagger & \mathbf{a}_1 \mathbf{a}_1^\dagger + \mathbf{b}_1 \mathbf{b}_1^\dagger & \mathbf{a}_1 \mathbf{b}_2^\dagger & 0 \\ 0 & \mathbf{b}_2 \mathbf{a}_1^\dagger & \mathbf{a}_2 \mathbf{a}_2^\dagger + \mathbf{b}_2 \mathbf{b}_2^\dagger & \mathbf{a}_2 \mathbf{b}_3^\dagger \\ \mathbf{a}_3 \mathbf{b}_0^\dagger & 0 & \mathbf{b}_3 \mathbf{a}_2^\dagger & \mathbf{a}_3 \mathbf{a}_3^\dagger + \mathbf{b}_3 \mathbf{b}_3^\dagger \end{pmatrix}. \quad (2-6)$$

The non-zero entries of $\mathbf{H}_M \mathbf{H}_M^\dagger$ are thus equal to

$$\begin{aligned} \left[\mathbf{H}_M \mathbf{H}_M^\dagger \right]_{m,m} &= \sum_{k=1}^K |a_{m,k}|^2 + \sum_{k=1}^K |b_{m,k}|^2 \\ \left[\mathbf{H}_M \mathbf{H}_M^\dagger \right]_{m,\widehat{m-1}} &= \sum_{k=1}^K a_{\widehat{m-1},k}^* b_{m,k} \\ \left[\mathbf{H}_M \mathbf{H}_M^\dagger \right]_{m,\widehat{m+1}} &= \sum_{k=1}^K a_{m,k} b_{\widehat{m+1},k}^* \end{aligned} \quad (2-7)$$

The average per-cell spectral efficiency in bits/sec/Hz, expressed as a function of the system average transmit E_b/N_0 , E_b^t/N_0 , is evaluated by solving the implicit equation obtained by substituting

$$\bar{P} = C_{\text{ul}} \left(\frac{E_b^t}{N_0} \right) \frac{E_b^t}{N_0} \quad (2-8)$$

in (2-3), where $C_{\text{ul}}(E_b^t/N_0) = C_{\text{ul}}(\bar{P})$ stands for the uplink spectral efficiency. Characterization of system performance in extreme SNR regimes is also of great interest. The low-SNR regime is characterized through the minimum transmit E_b/N_0 that enables reliable communications,

$$\frac{E_b^t}{N_{0 \min}} \triangleq \frac{\log_e 2}{\dot{C}_{\text{ul}}(0)}, \quad (2-9)$$

and the low-SNR spectral efficiency slope

$$S_0 \triangleq \frac{2 \left[\dot{C}_{\text{ul}}(0) \right]^2}{-\ddot{C}_{\text{ul}}(0)}, \quad (2-10)$$

yielding the following low-SNR approximation

$$C_{\text{ul}} \left(\frac{E_b^t}{N_0} \right) \approx \frac{S_0}{3|_{\text{dB}}} \left(\frac{E_b^t}{N_0} \Big|_{\text{dB}} - \frac{E_b^t}{N_{0 \min}} \Big|_{\text{dB}} \right). \quad (2-11)$$

In the above definitions $3|_{\text{dB}} = 10 \log_{10} 2$, and $\dot{C}_{\text{ul}}(0)$ and $\ddot{C}_{\text{ul}}(0)$ are the first and second derivatives (whenever exist) of the average per-cell sum-rate capacity with respect to \bar{P} , respectively, evaluated in nats/dimension at $\bar{P} = 0$. The high-SNR regime is characterized

through the high-SNR slope (also referred to as the “multiplexing gain”, or “pre-log”)

$$S_\infty \triangleq \lim_{\bar{P} \rightarrow \infty} \bar{P} \dot{C}_{\text{ul}}(\bar{P}) , \quad (2-12)$$

with $\dot{C}_{\text{ul}}(\bar{P})$ evaluated in nats/dimension, and the high-SNR power offset

$$\mathcal{L}_\infty \triangleq \lim_{\bar{P} \rightarrow \infty} \left(\log_2 \bar{P} - \frac{C_{\text{ul}}(\bar{P})}{S_\infty} \right) , \quad (2-13)$$

with $C_{\text{ul}}(\bar{P})$ evaluated in bits/dimension, yielding the following affine capacity approximation

$$C_{\text{ul}}(\bar{P}) \underset{\bar{P} \gg 1}{\approx} \frac{S_\infty}{3|_{\text{dB}}} (\bar{P}|_{\text{dB}} - 3|_{\text{dB}} \mathcal{L}_\infty) . \quad (2-14)$$

Note that the high-SNR approximation reference channel here is that of a single isolated cell, with no fading, and total average transmit power \bar{P} . The reader is referred to [14], [36], [37] for an elaboration on the extreme SNR characterization.

2.3 Non-Fading Channels

The case of non-fading channels is represented by setting $a_{m,k} = b_{m,k} = 1, \forall m, k$. Observing (2-7), it is clear that without fading the sum-rate capacity of (2-3) depends only on the total intra-cell transmit power \bar{P} (i.e., the sum of the intra-cell users’ powers). Hence, all transmission schemes with equal total intra-cell transmit power achieve the same throughput. In particular, the uplink average per-cell sum-rate capacity can be achieved by an intra-cell TDMA scheduling scheme, according to which there is only a single simultaneously active user in each cell, transmitting for a fraction $1/K$ of the time with power \bar{P} . It can also be equivalently achieved via a WB transmission scheme, according to which all users are simultaneously active, signaling each with power P . This equivalence, and the optimality of both transmission schemes (in the absence of fading), have been previously reported in [7] for a similar setting. The following propositions summarize the main results for the uplink channel in the absence of fading.

Proposition 2.1 *The uplink average per-cell sum-rate capacity in the absence of fading*

is given by

$$C_{\text{ul-nf}}(\bar{P}) = \frac{1}{M} \sum_{m=0}^{M-1} \log \left(1 + 2\bar{P} \left(1 + \cos \left(2\pi \frac{m}{M} \right) \right) \right) \quad (2-15)$$

$$\xrightarrow{M \rightarrow \infty} \log \left(\frac{1 + 2\bar{P} + \sqrt{1 + 4\bar{P}}}{2} \right) .$$

Proof: According to the underlying non-fading channel model, the matrix $\frac{1}{K} (\mathbf{H}_M \mathbf{H}_M^\dagger)$ is a circulant matrix with the non-zero row elements $\{1, 2, 1\}$. For example, for the particular case of $M = 4$ it is given by

$$\frac{1}{K} \mathbf{H}_4 \mathbf{H}_4^\dagger = \begin{pmatrix} 2 & 1 & 0 & 1 \\ 1 & 2 & 1 & 0 \\ 0 & 1 & 2 & 1 \\ 1 & 0 & 1 & 2 \end{pmatrix} . \quad (2-16)$$

The eigenvalues of $\frac{1}{K} (\mathbf{H}_M \mathbf{H}_M^\dagger)$ are hence [34]

$$\psi_m = 2 + 2 \cos \left(2\pi \frac{m}{M} \right) \quad ; \quad m = 0, 1, \dots, M-1 , \quad (2-17)$$

and since from (2-3) the average per-cell sum-rate capacity satisfies

$$C_{\text{ul-nf}}(\bar{P}) = \frac{1}{M} \sum_{m=0}^{M-1} \log (1 + \bar{P} \psi_m) , \quad (2-18)$$

the first equality in (2-15) follows immediately. Now taking the limit as the number of cells gets large, $M \rightarrow \infty$, the above result boils down to [34]

$$C_{\text{ul-nf}}(\bar{P}) = \lim_{M \rightarrow \infty} \frac{1}{M} \log \det \left(\mathbf{I}_M + \frac{\bar{P}}{K} \mathbf{H}_M \mathbf{H}_M^\dagger \right) \quad (2-19)$$

$$= \int_0^1 \log (1 + 2\bar{P} (1 + \cos (2\pi\theta))) d\theta ,$$

and the limiting result in (2-15) is due to [7]. ■

Proposition 2.2 *The uplink channel extreme-SNR regimes for non-fading channels and*

$M \geq 3$, are characterized by

$$\begin{aligned}
\frac{E_b^t}{N_{0\min}} &= \frac{\log_e 2}{2}; \\
S_0 &= \frac{4}{3}; \\
S_\infty &= \begin{cases} 1 & M \text{ odd} \\ \frac{M-1}{M} & M \text{ even} \end{cases} \xrightarrow{M \rightarrow \infty} 1; \\
\mathcal{L}_\infty &= \begin{cases} -1 - \frac{1}{M} \sum_{m=0}^{M-1} \log_2 \left(1 + \cos \left(\frac{2\pi m}{M} \right) \right) & M \text{ odd} \\ -\frac{(M-1)}{M} - \frac{1}{M} \sum_{\substack{m=0 \\ m \neq M/2}}^{M-1} \log_2 \left(1 + \cos \left(\frac{2\pi m}{M} \right) \right) & M \text{ even} \end{cases} \xrightarrow{M \rightarrow \infty} 0.
\end{aligned} \tag{2-20}$$

Proof: The proposition follows straightforwardly from (2-9), (2-10), (2-12), (2-13) and Proposition 2.1. ■

In order to gain more insight into the nature of the results, it is interesting to compare the results of Proposition 2.2 to the corresponding results for a single isolated cell (with total average transmit power \bar{P} , and non-fading channels), which serves here as a reference channel. It is well known (see [14], [36], [37]) that this channel is characterized in the extreme SNR regimes by

$$\begin{aligned}
\frac{E_b^t}{N_0} &= \log_e 2 \quad ; \quad S_0 = 2 \\
S_\infty &= 1 \quad ; \quad \mathcal{L}_\infty = 0.
\end{aligned} \tag{2-21}$$

In view of (2-21), it is observed that joint multi-cell processing yields a 3dB gain in the minimum transmit E_b/N_0 that enables reliable communications, in agreement with the underlying model according to which the signals are received by two cell-sites. Furthermore, although the low-SNR slope in the multi-cell setting is lower than the one obtained in a single isolated cell (4/3 vs. 2), the spectral efficiency in the multi-cell setting surpasses that of the single cell setting for $E_b^t/N_0 \lesssim 0.4\text{dB}$. In the high-SNR regime, where signals from neighboring cells become more dominant, the spectral efficiency in the multi-cell setting approaches that of the single cell setting as the number of cells M grows, however it is lower for any finite M .

2.4 Flat-Fading Channels

Introducing flat fading, the channel coefficients are taken as i.i.d. random variables, denoting by

$$\begin{aligned} m_1 &\triangleq E\{a_{m,k}\} = E\{b_{m,k}\} \quad ; \quad m_2 \triangleq E\{|a_{m,k}|^2\} = E\{|b_{m,k}|^2\} \\ m_4 &\triangleq E\{|a_{m,k}|^4\} = E\{|b_{m,k}|^4\} \quad ; \quad \mathcal{K} \triangleq \frac{m_4}{m_2^2} \quad , \quad \forall m, k \end{aligned} \quad (2-22)$$

the mean, second power moment, fourth power moment and the kurtosis of an individual fading coefficient. As above, both intra-cell TDMA and the WB scheme are considered, however in contrast to the results for non-fading channels, in the presence of fading the two schemes are no longer equivalent, as will be shown in the following.

2.4.1 Intra-Cell TDMA Scheduling

Particularizing to Rayleigh fading, $\{a_{m,k}\}, \{b_{m,k}\}, \forall m, k$ are taken as i.i.d. circularly symmetric complex Gaussian random variables with $m_1 = 0$ and $m_2 = 1$. Focusing on the large number of cells limit $M \rightarrow \infty$, the average per-cell sum-rate capacity with intra-cell TDMA is given by the following proposition.

Proposition 2.3 *The limiting average per-cell sum-rate capacity with intra-cell TDMA scheduling, as $M \rightarrow \infty$, is given by*

$$C_{tdma}(\bar{P}) = \int_1^\infty \log x \frac{\log_e(x) e^{-\frac{x}{\bar{P}}}}{\text{Ei}\left(\frac{1}{\bar{P}}\right) \bar{P}} dx \quad , \quad (2-23)$$

where $\text{Ei}(x) = \int_1^\infty \frac{\exp(-xt)}{t} dt$ is the exponential integral function.

Proof: The key tool for the derivation of (2-23) is a result by Narlua [35], obtained for the two taps time varying ISI channel. Considering i.i.d. zero-mean circularly symmetric complex Gaussian ISI coefficient, with unit variance, the capacity of the ISI channel is observed to be given by the limit of (2-3) as $M \rightarrow \infty$ (taking $K = 1$), with a slight modification of the structure of the transfer matrix \mathbf{H}_M . Accordingly, \mathbf{H}_M has a ‘‘Toeplitz-like’’ structure, which is completely equivalent to a modified cellular system model with cells ordered in a *linear* array (instead of a circular array), as considered for example in

[7], and with Rayleigh fading channels.

Following [35], the diagonal entries of \mathbf{D}_M in the Cholesky decomposition of the covariance matrix $\left(\mathbf{I}_M + \bar{P}\mathbf{H}_M\mathbf{H}_M^\dagger\right)\Big|_{K=1} = \mathbf{L}_M\mathbf{D}_M\mathbf{U}_M$ (where \mathbf{L}_M , \mathbf{D}_M , and \mathbf{U}_M denote a lower triangular matrix with unit diagonal entries, a diagonal matrix, and an upper triangular matrix with unit diagonal entries, respectively), are given by

$$d_m = 1 + \bar{P}|a_m|^2 + \bar{P}|b_m|^2 \left(1 - \bar{P}\frac{|a_{m-1}|^2}{d_{m-1}}\right), \quad m = 1, \dots, M-1, \quad (2-24)$$

with $d_0 = 1 + \bar{P}|a_0|^2 + \bar{P}|b_0|^2$. Remarkably, Narula has managed to prove that the diagonal entries $\{d_m\}$ may be viewed as a first order discrete-time continuous space Markov chain, with an ergodic stationary distribution given by

$$f_d(x) = \frac{\log_e(x)e^{-\frac{x}{\bar{P}}}}{\text{Ei}\left(\frac{1}{\bar{P}}\right)\bar{P}} \quad ; \quad x \geq 1. \quad (2-25)$$

Furthermore, it is shown in [35] that as $M \rightarrow \infty$, the strong law of large numbers (SLLN) holds for the sequence $\{\log d_m\}$, although the elements of $\{d_m\}$ are not independent. Hence, the average per-cell sum-rate capacity with intra-cell TDMA scheduling, in the framework of the modified linear array system model, can be written as

$$\begin{aligned} C_{\text{tdma}} &= \lim_{M \rightarrow \infty} E \left\{ \frac{1}{M} \log \det \left(\mathbf{I}_M + \bar{P}\mathbf{H}_M\mathbf{H}_M^\dagger\right)\Big|_{K=1} \right\} \\ &= \lim_{M \rightarrow \infty} E \left\{ \frac{1}{M} \log \det (\mathbf{L}_M\mathbf{D}_M\mathbf{U}_M) \right\} \\ &= \lim_{M \rightarrow \infty} E \left\{ \frac{1}{M} \sum_{m=0}^M \log d_m \right\} = E_d \{\log d\}, \end{aligned} \quad (2-26)$$

where the last expectation is taken with respect to $f_d(x)$, as defined in (2-25). Finally, using analogous arguments to the ones in [38], (2-26) can be shown to coincide, as $M \rightarrow \infty$, with the average per-cell sum-rate capacity of intra-cell TDMA scheduling in the original circular array system model. ■

The behavior of the intra-cell TDMA scheduling scheme in extreme-SNR regimes is summarized by the following proposition.

Proposition 2.4 *The uplink channel extreme-SNR regimes for Rayleigh-fading channels, and intra-cell TDMA scheduling, are characterized by*

$$\begin{aligned} S_0 &= 1 \quad ; \quad E_b^t/N_{0\min} = \frac{\log_e 2}{2} \\ S_\infty &= 1 \quad ; \quad \mathcal{L}_\infty \approx 0.84 . \end{aligned} \tag{2-27}$$

Proof: The results are derived by applying the basic definitions of $E_b^t/N_{0\min}$, S_0 , S_∞ and \mathcal{L}_∞ , as in Subsection 2.2, to (2-26). The high-SNR regime is characterized employing symbolic mathematical software tools. ■

It is now of interest to compare the results of Propositions 2.3 and 2.4, to the corresponding results of Subsection 2.3 for non-fading channels. Using another result from [35], the following relation between the average per-cell sum-rate capacities for the two channel models is derived.

Proposition 2.5 *The presence of Rayleigh fading reduces the average per-cell sum-rate capacity of the intra-cell TDMA scheduling scheme*

$$C_{tdma}(\bar{P}) \leq C_{ul-nf}(\bar{P}) . \tag{2-28}$$

Proof: See Appendix A. ■

It is important to emphasize at this point that the above relation does not hold in general. Rather, it is an outcome of the particular multi-cell model considered here, according to which the cell-sites are located at the cells' boundaries. For example, in the linear cell-array model suggested by Wyner in [7], where the cell-sites are located at the cells' centers, the relation between the sum-rate capacities, with and without fading, may be reversed under certain conditions [9], depending on the out-of-cell interference factor. Examining the extreme-SNR regimes, it is observed that in the low-SNR regime Rayleigh fading reduces the slope of the spectral efficiency (from 4/3 to 1), while the minimum transmit E_b/N_0 that enables reliable communications is identical in both cases. In the high-SNR regime the impact of Rayleigh fading is observed in the power offset ($\mathcal{L}_\infty = 0.84$ vs. $\mathcal{L}_\infty = 0$ for $M \rightarrow \infty$ and no-fading), while the high-SNR slope, or multiplexing gain, is unaffected by the presence of Rayleigh fading.

2.4.2 WB Scheme

Considering the WB scheme, with all users simultaneously active, the focus is on the large number of users per cell setting $K \gg 1$. As in [9], applying the SLLN as K increases, while keeping the total per-cell transmit power \bar{P} constant, the diagonal entries of $\frac{1}{K}\mathbf{H}_M\mathbf{H}_M^\dagger$ (see (2-3)) are given by

$$\left[\frac{1}{K}\mathbf{H}_M\mathbf{H}_M^\dagger\right]_{m,m} = \frac{1}{K} \left(\sum_{k=1}^K |a_{m,k}|^2 + \sum_{k=1}^K |b_{m,k}|^2 \right) \xrightarrow{SLLN} 2E\{|a|^2\} = 2m_2, \quad (2-29)$$

where a represents a random variable with the distribution of an individual fading coefficient (see (2-22)). Similarly, the non-zero off-diagonal entries of $\frac{1}{K}\mathbf{H}_M\mathbf{H}_M^\dagger$ satisfy

$$\begin{aligned} \left[\frac{1}{K}\mathbf{H}_M\mathbf{H}_M^\dagger\right]_{m,\widehat{m-1}} &= \frac{1}{K} \sum_{k=1}^K a_{\widehat{m-1},k}^* b_{m,k} \xrightarrow{SLLN} |E\{a\}|^2 = |m_1|^2 \\ \left[\frac{1}{K}\mathbf{H}_M\mathbf{H}_M^\dagger\right]_{m,\widehat{m+1}} &= \frac{1}{K} \sum_{k=1}^K a_{m,k} b_{\widehat{m+1},k}^* \xrightarrow{SLLN} |E\{a\}|^2 = |m_1|^2 \end{aligned} \quad (2-30)$$

Hence, the covariance matrix $\frac{1}{K}\mathbf{H}_M\mathbf{H}_M^\dagger$ converges as $K \rightarrow \infty$ to a circulant matrix. For example, with $M = 4$

$$\frac{1}{K}\mathbf{H}_4\mathbf{H}_4^\dagger \xrightarrow{SLLN} \begin{pmatrix} 2m_2 & |m_1|^2 & 0 & |m_1|^2 \\ |m_1|^2 & 2m_2 & |m_1|^2 & 0 \\ 0 & |m_1|^2 & 2m_2 & |m_1|^2 \\ |m_1|^2 & 0 & |m_1|^2 & 2m_2 \end{pmatrix}. \quad (2-31)$$

Proposition 2.6 *The uplink average per-cell sum-rate capacity while employing the WB scheme is given by*

$$\begin{aligned} C_{wb}(\bar{P}) &= \frac{1}{M} \sum_{m=0}^{M-1} \log \left(1 + 2\bar{P} \left(m_2 + |m_1|^2 \cos \left(2\pi \frac{m}{M} \right) \right) \right) \\ &\xrightarrow{M \rightarrow \infty} \log \left(\frac{1 + 2\bar{P}m_2 + \sqrt{1 + 4\bar{P}m_2 + 4\bar{P}^2(m_2^2 - |m_1|^4)}}{2} \right). \end{aligned} \quad (2-32)$$

Proof: Due to the limiting circulant structure, as $K \rightarrow \infty$, the eigenvalues of $\frac{1}{K}\mathbf{H}_M\mathbf{H}_M^\dagger$ are given by [34]

$$\psi_m = 2m_2 + 2|m_1|^2 \cos\left(2\pi\frac{m}{M}\right) \quad ; \quad m = 0, 1, \dots, M-1. \quad (2-33)$$

Since the average per-cell sum-rate capacity equals

$$C_{\text{wb}}(\bar{P}) = \frac{1}{M} \sum_{m=0}^{M-1} \log(1 + \bar{P}\psi_m), \quad (2-34)$$

the first equality in (2-32) follows immediately by substituting (2-33) into (2-34). Taking the number of cells M to infinity yields

$$\begin{aligned} C_{\text{wb}}(\bar{P}) &= \lim_{M \rightarrow \infty} \frac{1}{M} \log \det \left(\mathbf{I}_M + \frac{\bar{P}}{K} \mathbf{H}_M \mathbf{H}_M^\dagger \right) \\ &= \int_0^1 \log(1 + 2\bar{P}(m_2 + |m_1|^2 \cos(2\pi\theta))) d\theta \\ &= \log \left(\frac{1 + 2\bar{P}m_2 + \sqrt{1 + 4\bar{P}m_2 + 4\bar{P}^2(m_2^2 - |m_1|^4)}}{2} \right), \end{aligned} \quad (2-35)$$

where the last equality is due to Wyner [7]. This completes the proof. ■

Now examining the limiting expression in (2-32), it is easy to verify that fixing the second power moment of the fading distribution m_2 , $C_{\text{wb}}(\bar{P})$ is a decreasing function of $|m_1|^2$. Hence, zero mean fading distributions produce the highest average per-cell sum-rate capacity, and in such case

$$C_{\text{wb}}(\bar{P}) = \log(1 + 2\bar{P}m_2). \quad (2-36)$$

For the particular case of Rayleigh fading, $m_2 = 1$, (2-36) reduces to

$$C_{\text{wb}}(\bar{P}) = \log(1 + 2\bar{P}), \quad (2-37)$$

which exhibits the full diversity scale of the multi-cell system model in concern, while out-of-cell interference is completely eliminated. The resulting sum-rate capacity is equivalent to the one of a single isolated cell without fading, but with twice the SNR.

The average per-cell sum-rate capacity in the absence of fading, as given by Proposition 2.1, can be obtained as a particular case of (2-32), while substituting $m_1 = m_2 = 1$. Comparing the results, it is observed that in the large number of users per cell limit, the presence of fading turns out beneficial in terms of the average per-cell sum-rate capacity. This performance enhancement is due to the independency of the two fading processes affecting the signal of each user, as observed by the two receiving cell sites, which explains why mimicking artificial fading at the users' transmitters fails to produce the same impact [9]. In addition, adhering to similar arguments as in [9], it can be shown that in the presence of fading the WB scheme outperforms the intra-cell TDMA scheme, and that the two expressions in (2-32) also upper bound the average per-cell sum-rate capacity for any *finite* number of users per cell.

The extreme-SNR behavior of the WB scheme is summarized in the following propositions. Their proofs follow straightforwardly by applying the basic definitions of $E_b^t/N_{0\min}$, S_0 , S_∞ and \mathcal{L}_∞ to (2-32).

Proposition 2.7 *For a general fading distribution, as defined in (2-22), $\forall K > 0$, and $\forall M \geq 3$, the uplink average per-cell sum-rate capacity in the low-SNR regime with the WB scheme is characterized by*

$$\frac{E_b^t}{N_{0\min}} = \frac{\log_e 2}{2m_2} \quad ; \quad S_0 = \frac{2}{\frac{\mathcal{K}}{2K} + \frac{|m_1|^4}{2m_2^2} + 1} . \quad (2-38)$$

Proposition 2.8 *For a general fading distribution, as defined in (2-22), for $K \gg 1$, and $\forall M \geq 3$, the uplink average per-cell sum-rate capacity in the high-SNR regime with the WB scheme is characterized by*

$$\begin{aligned} S_\infty &= 1 \\ \mathcal{L}_\infty &= -1 - \frac{1}{M} \sum_{m=0}^{M-1} \log_2 \left(m_2 + |m_1|^2 \cos \left(\frac{2\pi m}{M} \right) \right) \\ &\xrightarrow{M \rightarrow \infty} -\log_2 \left(m_2 + \sqrt{m_2^2 - |m_1|^4} \right) . \end{aligned} \quad (2-39)$$

The extreme-SNR behavior for the particular case of Rayleigh fading is summarized next.

Proposition 2.9 *For Rayleigh fading, $K \gg 1$, and $\forall M \geq 3$, the uplink average per-cell sum-rate capacity in extreme-SNR regimes with the WB scheme is characterized by*

$$\begin{aligned} \frac{E_b^t}{N_{0 \min}} &= \frac{\log_e 2}{2} \quad ; \quad S_0 = 2 \\ S_\infty &= 1 \quad ; \quad \mathcal{L}_\infty = -1 . \end{aligned} \tag{2-40}$$

In view of Propositions 2.7–2.9, comparing the results for Rayleigh fading to the corresponding results of Propositions 2.2 and 2.4, one can conclude the following. In the low-SNR regime, the minimum transmit E_b/N_0 that enables reliable communications is identical for either intra-cell TDMA or the WB scheme, with or without fading. However in the presence of Rayleigh fading, employing the WB scheme with more than two simultaneously active users per cell ($K > 2$), produces a higher low-SNR slope, and hence a higher spectral efficiency, as compared to result for non fading channels, and also for intra-cell TDMA scheduling ($K = 1$). Turning to the high-SNR regime, it is observed that the WB scheme produces the same multiplexing gain (or high-SNR slope) as the one obtained with intra-cell TDMA, and in the absence of fading. However, the WB scheme produces an ≈ 5.52 dB high-SNR power offset advantage over intra-cell TDMA with Rayleigh fading, and a 3dB advantage over the corresponding result for non-fading channels.

2.5 Numerical Results

Some numerical results for the uplink channel are shown in Figs. 2–6. Fig. 2 shows the average per-cell sum-rate capacity as a function of the total intra-cell transmit SNR \bar{P} . The sum-rate capacity for non-fading channels is included in the figure, as well as for the intra-cell TDMA and WB schemes in Rayleigh fading channels. The corresponding spectral efficiencies are plotted in Fig. 3 as a function of E_b^t/N_0 . The results in both figures are for the case in which the number of cells is large $M \gg 1$. The figures demonstrate the inferiority of intra-cell TDMA scheduling in the presence of Rayleigh fading, as compared to the case of non fading channels, and to the WB scheme in the presence of fading (producing the highest performance). Examining the results at the low- and high-SNR regimes reveals, in general, a good match to the results of propositions 2.2, 2.4 and 2.9. It is noted however that the numerically evaluated high-SNR power offset \mathcal{L}_∞ for intra-cell TDMA scheduling,

is smaller than the value specified in proposition 2.4. This value is closely approached only for very high values of \bar{P} .

Fig. 4 shows the impact of the number of cells on system performance. Assuming no fading, the uplink average per-cell sum-rate capacity is plotted for several values of the total intra-cell transmit SNR, \bar{P} , as function of the number of system cells. A “relaxed oscillatory” behavior is observed in the figure as the number of cells increases. Furthermore, it is also observed that the convergence rate is faster for lower values of \bar{P} , and that for any practical purposes a system composed of at least 30 cells may be treated as an “infinite” dimensional system.

Finally, the validity of the limiting result in (2-32) is also examined. Recall that this result was shown to approximate the average per-cell sum-rate capacity of the WB scheme (Rayleigh fading) in the case in which the number of users per cell is large, and it provides an upper bound to the sum-rate capacity for any finite number of users per cell. In order to validate the approximation, the limiting ($K \gg 1$, $M \gg 1$) capacity and spectral efficiency are plotted in Figs. 5 and 6 together with Monte-Carlo simulation results. The Monte-Carlo simulations were performed while assuming a finite dimensional system of $M = 30$ cells (demonstrated in Fig. 4 to be large enough), and while employing the WB scheme with $K = 1$ (corresponding to intra-cell TDMA), $K = 2$ and $K = 4$ users per cell. It is observed that the asymptotic expression indeed upper bounds the results obtained with a finite number of users per cell. Furthermore, it also provides a very tight approximation for system performance even with very modest numbers of users per cell. It is also observed that the WB scheme is superior to intra-cell TDMA scheduling for even as low as 2 users per cells.

3 Downlink Sum-Rate Capacity

3.1 Preliminaries and Downlink System Model

The key tool used in the analysis to follow is a recent result by Yu and Lan [3], who established a connection between the uplink-downlink duality of the Gaussian vector MAC and BC, and the Lagrangian duality in minimax optimization. The main result of [3] is therefore reviewed first. The setup considered in [3] is a memoryless Gaussian vector

BC, that models the downlink of a wireless single-cell system with N antennas at the cell-site, and K single antenna users. Considering an arbitrary time instance, the baseband representation of the $K \times 1$ received signal vector is given by

$$\mathbf{y}_{dl} = \mathcal{H}^\dagger \mathbf{x}_{dl} + \mathbf{z}_{dl}, \quad (3-1)$$

where \mathcal{H}^\dagger is a fixed $K \times N$ matrix with $[\mathcal{H}^\dagger]_{i,j}$ denoting the channel gain from the i th antenna at the cell-site to the j th user. Full channel state information is assumed available to both transmitter and receivers. \mathbf{x}_{dl} is the $N \times 1$ input vector for which an individual per-antenna power constraint of $[\text{cov}(\mathbf{x}_{dl})]_{(i,i)} \leq P_i$ is assumed. \mathbf{z}_{dl} is a $K \times 1$ circularly symmetric zero mean complex AWGN vector, with identity covariance matrix. It is worth mentioning that for $N > 1$ this is a non-degraded Gaussian BC, the capacity region of which was recently shown in [27] to coincide with the DPC achievable rate region [23] [5] [6]. One of the main results of [3] is the following Theorem.

Theorem 3.1 (Yu and Lan (2004)) *The sum capacity of the Gaussian multi-antenna BC with individual per antenna transmit power constraints $[\text{cov}(\mathbf{x}_{dl})]_{(n,n)} \leq P_n$ is the same as the sum capacity of a dual MAC with a sum power constraint and with a diagonal and “uncertain” noise:*

$$C_{sum} = \min_{\mathbf{\Lambda}} \max_{\mathcal{D}} \log \frac{\det(\mathcal{H}\mathcal{D}\mathcal{H}^\dagger + \mathbf{\Lambda})}{\det(\mathbf{\Lambda})},$$

such that \mathcal{D} and $\mathbf{\Lambda}$ are $K \times K$ and $N \times N$ nonnegative diagonal matrices, satisfying $\text{Tr}(\mathcal{D}) \leq 1$ and $\sum_n P_n [\mathbf{\Lambda}]_{(n,n)} \leq 1$, respectively.

Accordingly, the sum-rate capacity of the downlink (broadcast) channel equals the sum-rate capacity of its dual uplink (multiple access) channel, subject to a joint power constraint determining the level of cooperation between the users, and a noise power constraint capturing the individual per-antenna power constraints of the original downlink (broadcast) channel.

Now it easily observed that Theorem 3.1 directly applies to the circular cell-array system model considered here, by viewing the cell-sites as a single distributed antenna array. This observation shall be used in the rest of this section. Accordingly, focusing on an arbitrary time instance, the received signal vector is given by (3-1) while replacing N , K , and \mathcal{H} by

M , MK , and \mathbf{H}_M (as defined by (2-2)), respectively, i.e.,

$$\mathbf{y}_{dl} = \mathbf{H}_M^\dagger \mathbf{x}_{dl} + \mathbf{z}_{dl} . \quad (3-2)$$

With the natural analogy to the uplink channel, \mathbf{a}_m and \mathbf{b}_m of (2-2) are now $1 \times K$ row vectors denoting the channel complex fading coefficients, experienced by the K users of the m th and $[(m-1) \bmod M]$ th cells, respectively, when receiving the transmissions of the m th cell-site antenna. As for the uplink channel, it is also assumed here that the fading processes are i.i.d. among different users, and can be viewed for each user as an ergodic process with respect to the time index. Full channel state information (CSI) is assumed available to the joint multi-cell transmitter, while the mobile receivers are assumed to be cognizant of their own CSI, and of the employed transmission strategy. \mathbf{x}_{dl} is the $M \times 1$ vector of signals transmitted by the M cell-sites, for which an *equal individual per-cell-site power constraint* of $[\text{cov}(\mathbf{x}_{dl})]_{(m,m)} \leq \bar{P} \forall m$ is assumed. \mathbf{z}_{dl} is an $MK \times 1$ circularly symmetric zero mean complex AWGN vector, with identity covariance matrix, representing the noises at the receivers of each of the users. Using Theorem 3.1 the downlink average per-cell sum-rate capacity is given by

$$C_{dl}(\bar{P}) = E_{H_M} \left\{ \frac{1}{M} \min_{\mathbf{\Lambda}_M} \max_{\mathbf{D}_M} \log \frac{\det(\mathbf{H}_M \mathbf{D}_M \mathbf{H}_M^\dagger + \mathbf{\Lambda}_M)}{\det(\mathbf{\Lambda}_M)} \right\} , \quad (3-3)$$

where the optimization is over all nonnegative diagonal matrices $\mathbf{D}_{M[MK \times MK]}$ and $\mathbf{\Lambda}_{M[M \times M]}$, satisfying $\text{Tr}(\mathbf{D}_M) \leq 1$ and $\text{Tr}(\mathbf{\Lambda}_M) \leq 1/\bar{P}$, respectively (note the minimization in (3-3), that addresses the *equal* individual per-cell average power constraints). The average per-cell spectral efficiency can be evaluated using the same approach as in Subsection 2.2.

3.2 Dual Uplink System Model

Since Theorem 3.1 gives the sum-rate capacity of the downlink channel in terms of a minimax optimization on the dual uplink channel, the focus in the sequel will be on the dual channel, which in the multi-cell setting considered here is given by

$$\tilde{\mathbf{y}}_{ul} = \mathbf{H}_M \tilde{\mathbf{x}}_{ul} + \tilde{\mathbf{z}}_{ul} . \quad (3-4)$$

The $(\tilde{\cdot})$ notation was introduced here to emphasize the difference between the *dual* uplink channel and the actual uplink channel of the multi-cell system, as described in Subsection 2.2. The $M \times KM$ channel transfer matrix \mathbf{H}_M of the dual uplink channel is as defined in (2-2). In view of Theorem 3.1, the diagonal $MK \times MK$ input covariance matrix can be written as

$$\mathbf{D}_M = \text{diag}(\mathbf{D}_0, \mathbf{D}_1, \dots, \mathbf{D}_{M-1}), \quad (3-5)$$

where \mathbf{D}_m is a $K \times K$ non-negative diagonal matrix representing the transmit powers of the m th cell's users. The nonzero entries of \mathbf{D}_m are denoted by $\{d_{m,k}\}_{k=1}^K$. As stated in the pervious subsection, the individual power constraints corresponding to the original downlink (broadcast) channel are assumed to be all equal to \bar{P} .

Combining (2-2) and (3-5), it follows that the matrix product $\mathbf{H}_M \mathbf{D}_M \mathbf{H}_M^\dagger$ of (3-3) is an $M \times M$ matrix given by

$$\left[\mathbf{H}_M \mathbf{D}_M \mathbf{H}_M^\dagger \right]_{m,n} = \begin{cases} \mathbf{a}_m \mathbf{D}_m \mathbf{a}_m^\dagger + \mathbf{b}_m \mathbf{D}_{\widehat{m-1}} \mathbf{b}_m & n = m \\ \mathbf{b}_m \mathbf{D}_{\widehat{m-1}} \mathbf{a}_{\widehat{m-1}}^\dagger & n = \widehat{m-1} \\ \mathbf{a}_m \mathbf{D}_m \mathbf{b}_{\widehat{m+1}}^\dagger & n = \widehat{m+1} \\ 0 & \text{otherwise} \end{cases} \quad m = 0, 1, \dots, (M-1). \quad (3-6)$$

For example, in the particular case of $M = 4$

$$\mathbf{H}_4 \mathbf{D}_4 \mathbf{H}_4^\dagger = \begin{pmatrix} \mathbf{a}_0 \mathbf{D}_0 \mathbf{a}_0^\dagger + \mathbf{b}_0 \mathbf{D}_3 \mathbf{b}_0^\dagger & \mathbf{a}_0 \mathbf{D}_0 \mathbf{b}_1^\dagger & 0 & \mathbf{b}_0 \mathbf{D}_3 \mathbf{a}_3^\dagger \\ \mathbf{b}_1 \mathbf{D}_0 \mathbf{a}_0^\dagger & \mathbf{a}_1 \mathbf{D}_1 \mathbf{a}_1^\dagger + \mathbf{b}_1 \mathbf{D}_0 \mathbf{b}_1^\dagger & \mathbf{a}_1 \mathbf{D}_1 \mathbf{b}_2^\dagger & 0 \\ 0 & \mathbf{b}_2 \mathbf{D}_1 \mathbf{a}_1^\dagger & \mathbf{a}_2 \mathbf{D}_2 \mathbf{a}_2^\dagger + \mathbf{b}_2 \mathbf{D}_1 \mathbf{b}_2^\dagger & \mathbf{a}_2 \mathbf{D}_2 \mathbf{b}_3^\dagger \\ \mathbf{a}_3 \mathbf{D}_3 \mathbf{b}_0^\dagger & 0 & \mathbf{b}_3 \mathbf{D}_2 \mathbf{a}_2^\dagger & \mathbf{a}_3 \mathbf{D}_3 \mathbf{a}_3^\dagger + \mathbf{b}_3 \mathbf{D}_2 \mathbf{b}_3^\dagger \end{pmatrix}. \quad (3-7)$$

In a similar manner to (2-7), the non-zero entries of $\mathbf{H}_M \mathbf{D}_M \mathbf{H}_M^\dagger$ are explicitly expressed

by

$$\begin{aligned}
\left[\mathbf{H}_M \mathcal{D}_M \mathbf{H}_M^\dagger \right]_{m,m} &= \sum_{k=1}^K d_{m,k} |a_{m,k}|^2 + \sum_{k=1}^K d_{\widehat{m-1},k} |b_{m,k}|^2 \\
\left[\mathbf{H}_M \mathcal{D}_M \mathbf{H}_M^\dagger \right]_{m,\widehat{m-1}} &= \sum_{k=1}^K d_{\widehat{m-1},k} a_{\widehat{m-1},k}^* b_{m,k} \\
\left[\mathbf{H}_M \mathcal{D}_M \mathbf{H}_M^\dagger \right]_{m,\widehat{m+1}} &= \sum_{k=1}^K d_{m,k} a_{m,k}^* b_{\widehat{m+1},k}
\end{aligned} \tag{3-8}$$

The above explicit formulation will be useful in the analysis to follow.

3.3 Non-Fading Channels

For non-fading channels, taking $a_{m,k} = b_{m,k} = 1 \forall m, k$ as in Subsection 2.3, the downlink average per-cell sum-rate capacity is specified by the following proposition.

Proposition 3.2 *The downlink average per-cell sum-rate capacity in the absence of fading, with an equal individual per-cell power constraint \bar{P} , coincides with corresponding result for the uplink channel as stated by Proposition 2.1, i.e.,*

$$C_{dl-nf}(\bar{P}) = C_{ul-nf}(\bar{P}) . \tag{3-9}$$

Proof: See Appendix B. ■

Noting that for non-fading channels, the channel transfer matrix \mathbf{H}_M , as defined in (2-2), becomes block-circulant (circulant for $K = 1$), it is worth emphasizing that the arguments used to prove Proposition 3.2 (see Appendix B) hold verbatim for *any* block-circulant channel transfer matrix (as it is only the circular structure of \mathbf{H}_M that was used, and not the particular values of its entries in the model considered here). It can therefore be concluded that for *any block-circulant channel transfer matrix* the downlink average per-cell sum-rate capacity is equal to the average per-cell sum-rate capacity of its corresponding uplink channel with equal transmit powers. Furthermore, this result holds for either equal individual per cell-site (antenna) power constraints, or for a sum power constraint. In view of the above, the downlink average per-cell sum-rate capacity in extreme-SNR regimes is characterized by Proposition 2.2.

Deriving explicit expression for the downlink average per-cell sum-rate capacity, it is also of interest to identify a *downlink* transmission scheme that actually achieves this result. Note here that the sum-rate capacity was obtained through the dual *uplink* channel, however the dual uplink channel by itself does not directly specify a *downlink* transmission scheme that achieves the same capacity. In order to find such a scheme, one can use the uplink-downlink duality again, but this time in the “opposite direction”. In [6], a MAC-to-BC transformation is proposed that finds, for any ordering of the users in the MAC channel, and for rates obtained by means of successive cancellation at the receiver, a set of downlink transmit covariance matrices (per each of the users) that achieve the same rates per user by means of successive pre-cancellation at the transmitter (with *reverse* ordering), based on DPC. Say, for example, that one desires to find a downlink transmission scheme that is sum-rate optimum, and provides equal rates (say, for the case in which a single user is active in each cell, which is also sum-rate optimum for non-fading channels, as shown in Appendix B). Then, the above transformation can be employed for our setting in the following manner. Ordering the users by increasing cell indices, and assuming equal powers in the dual uplink channel, one can find the corresponding transmit covariance matrices that will achieve the same rates at the downlink. These rates define points in the uplink (MAC) and downlink capacity regions, corresponding to a set of non-equal rates (in view of the successive cancellation process) achieving the sum-rate capacity. The final step is to use equal time sharing of all possible cyclic shifts on the users’ ordering, which will finally provide equal rates for all users.

3.4 Rayleigh Flat-Fading Channels

Particularizing to Rayleigh fading lower and upper bounds for the downlink average per-cell sum-rate capacity are derived, while focusing on the asymptotic regime in terms of the number of users per cell $K \gg 1$. The following includes a short outline of the techniques by which the bounds are derived, while the reader is referred to Appendix C for the full detailed proofs.

The lower bound (achievable rate) is obtained by examining the dual uplink channel via (3-3). A “*Threshold Crossing*” (TC) scheduling scheme is employed, according to which only users received in the *dual* uplink channel, at *both* cell-sites, with fade power levels

exceeding some constant L , are allowed to transmit. As $K \rightarrow \infty$ the number of active users per cell crystalizes to $K_0 \triangleq Ke^{-2L}$, and it is assumed that all active users transmit at equal powers $1/(K_0M)$, to meet the power constraint of (3-3). Furthermore, the constant L should be chosen so that $K_0 \rightarrow \infty$ as $K \rightarrow \infty$ (and thus the strong law of large numbers can be applied). In particular, the achievable rate lower bound is obtained by choosing $K_0 = Ke^{-2L} = K^\epsilon$, yielding $L = \frac{1-\epsilon}{2} \log_e K$, where $0 < \epsilon < 1$. The resulting achievable rate can also be shown to constitute an upper bound for the rate attained with *any finite* K , while employing the TC scheduling scheme in the dual uplink (see Appendix C).

The key tool for deriving the capacity upper bound, is bounding the channel fades by the strongest fading gain (over all intra-cell users) received at each cell-site, and observing that the maximum of K i.i.d. $\chi^2(2)$ distributed random variables behaves like $f(K) \triangleq \log_e K + O(\log_e \log_e K)$ for $K \gg 1$ [39]. The two bounds are summarized in the following proposition *while ignoring little orders of $\log_e K$* .

Proposition 3.3 *For $K \gg 1$ the downlink average per-cell sum-rate capacity for Rayleigh fading satisfies*

$$\log(1 + \bar{P}((1 - \epsilon) \log_e K + 2)) \leq C_{dl}(\bar{P}) \leq \log(1 + 2\bar{P} \log_e K) \quad , \quad 0 < \epsilon < 1. \quad (3-10)$$

Proof: See Appendix C. ■

As can be observed, the above bounds are rather tight, and for $\epsilon \ll 1$ the gap between the two bounds is less than 1 [bit/sec/Hz] in the high-SNR region. Also, it is observed from the lower bound that, at least, a multiuser diversity gain factor proportional to $\log_e K$ can be achieved, and this comes in addition to the inherent system array diversity gain factor of two. One can conclude from the two bounds that the downlink average per-cell sum-rate capacity scales like $\log \log_e K$ in the large number of users per cell regime. The same scaling law has also been reported before for the single-cell setting with multiple antennas at the cell-site, as for example in [39] [40]. Note however that in this single-cell setting there is a full symmetry in the manner that each of the users “sees” the transmit antennas, where as in the multi-cell model considered here each of the users “sees” only two of the total of M system cell-sites.

The extreme SNR behavior of the two bounds is summarized next.

Proposition 3.4 *The downlink channel extreme-SNR regimes for Rayleigh fading are characterized, for any number of cells $M \geq 3$, by*

$$\begin{aligned}
 S_0 &= 2 ; \quad \frac{\log_e 2}{2 \log_e K} \leq \frac{E_b^t}{N_{0 \min}} \leq \frac{\log_e 2}{(1 - \epsilon) \log_e K + 2} \\
 S_\infty &= 1 ; \quad -1 - \log_2 \log_e K \leq \mathcal{L}_\infty \leq -\log_2 ((1 - \epsilon) \log_e K + 2) .
 \end{aligned}
 \tag{3-11}$$

Comparing the above results to the corresponding results in the absence of fading, as stated by Proposition 3.2, the beneficial effect of fading on the downlink average per-cell sum-rate capacity is clearly evident. Focusing on extreme-SNR regimes, it is observed that in the low-SNR regime the minimum transmit E_b/N_0 that enables reliable communication is decreased at least by a factor of $2/((1 - \epsilon) \log_e K + 2)$, while the low-SNR slope is increased by a factor of 1.5 (a slope of 2 vs. 4/3). In the high-SNR regime it is observed that the introduction of fading does not change the high-SNR slope (multiplexing gain). However, the power offset \mathcal{L}_∞ is lower by at least $\log_2 ((1 - \epsilon) \log_e K + 2)$ in the presence of fading.

In the context of the dual uplink channel, and in view of the TC scheduling scheme used to derive the lower bound on the downlink average per-cell sum-rate capacity, it is also interesting to note that setting the threshold to zero, and letting all users transmit simultaneously with equal powers, produces an achievable average per-cell sum-rate as given by (2-37). Comparing this result to the lower bound in (3-10), it is observed that the latter scheme fails to produce the multiuser diversity gain factor of $(1 - \epsilon) \log_e K$. It is important to emphasize however that (2-37) was derived while assuming no CSI is available to the transmitting users, whereas the TC scheduling scheme does require threshold crossing indication feedback from the receiving cell-sites. It is also worth noting in this respect that in the single-cell multiple antenna setting with Rayleigh fading, while assuming full CSI is available at both transmitting and receiving ends, the sum-rate optimum transmission strategy is bounded to include no more than M^2 simultaneously active users in either uplink or downlink channels (where M is the number of antennas at the cell-site) [41] [42]. Hence simultaneously transmitting to all $K \gg M^2$ users is definitely suboptimum.

As discussed in Subsection 3.3, the TC scheduling scheme introduced here for the dual uplink channel can also be employed to define a downlink DPC based transmission scheme that achieves the corresponding sum-rate. This can be accomplished again via the MAC-to-BC transformations suggested in [6]. Finally, it is noted that the results presented in

this section for Rayleigh fading may be extended in a straightforward manner to other fading distributions (although these may yield less compact and analytically tractable expressions).

3.5 Numerical Results

Numerical results for the downlink channel are shown in Figs. 7–10. Figs. 7–8 show the analytically derived lower and upper bounds for the downlink average per-cell sum-rate capacity, as given by Proposition 3.3, plotted as a function of the total transmit power (SNR) per cell \bar{P} , for $K = 100$. Fig. 7 shows the lower bound for $\epsilon = 0.4$, while Fig. 8 shows the bound for $\epsilon = 0.2$. In addition, the corresponding results of Monte-Carlo simulations (considering a system of $M = 30$ cells, see Subsection 2.5) of the dual uplink TC scheduling scheme, employed to obtain the lower bound on the sum-rate capacity, are also included, as well as the corresponding result for non-fading channels (2-19). The impact of multiuser diversity in the presence of fading on system performance is clearly demonstrated in the figures, comparing the results for non-fading and Rayleigh fading channels. It is also observed that even for a moderate number of users per cell ($K = 100$ in this case), the bounds are tight, resulting in less than one bit per channel use over the whole plotted SNR range. The gap between the two bounds reduces when the threshold parameter ϵ decreases, as may be concluded from (3-10). Furthermore, the Monte-Carlo simulation curves demonstrate a good match to the analytical lower bound for even as low as $K = 100$ users per cell. Note, that the Monte-Carlo curves are closer to the analytical bound for higher values of the threshold parameter ϵ . This is since for a fixed K , a higher value of ϵ implies that more users per cell are likely to experience threshold crossing fading coefficients, and therefore the SLLN based lower bound forms a better approximation for the finite number of users per cell setting. Note in this respect that the probability that *at least one* of the users at a given cell crosses the threshold is $1 - (1 - 1/K^{(1-\epsilon)})^K$, which for $K = 100$ equals ≈ 0.9985 when $\epsilon = 0.4$, and ≈ 0.9214 when $\epsilon = 0.2$. The analytical bounds are however further apart for lower values of ϵ . Figs. 9–10 show the corresponding downlink average per-cell spectral efficiency results, plotted as a function of the system average transmit E_b/N_0 . The beneficial effect of fading on system performance is again clearly demonstrated, and a good match to the low-SNR regime characterization

of Proposition 3.4 is observed.

It is important to note at this point, that the TC scheduling scheme employed here for deriving a lower bound to the downlink average per-cell sum-rate capacity, is also a legitimate scheduling scheme for the *original* uplink channel, provided that the system design allows such a scheme to be employed. So although not in the main focus of this research, it is of interest to demonstrate the impact of employing different scheduling schemes in the uplink of the cellular system model in concern. Fig. 11 compares the spectral efficiency results of the Monte-Carlo simulation of the TC scheme (performed taking $K = 100$, $\epsilon = 0.2$, and $M = 30$, as in Fig. 10), to the spectral efficiency of the WB scheme considered earlier in Subsection 2.4. As mentioned in the previous subsection the latter scheme also produces an achievable rate lower bound to the downlink average per-cell sum-rate capacity, although it is obviously a worse lower bound. Also included in this figure are Monte-Carlo simulation results of an “opportunistic” intra-cell TDMA scheduling scheme, according to which only the user with the maximum total received power, at both cell-sites, is allowed to transmit in each cell (i.e., the user corresponding to $\arg \max_k \{ |a_{m-1,k}|^2 + |b_{m,k}|^2 \}$), and this user transmits with the total intra-cell transmit power \bar{P} . The noise covariance matrix here was taken to be the identity matrix, and it is noted that this scheme cannot be regarded as providing an achievable rate lower bound for the downlink average per-cell sum-rate capacity with *equal individual per-cell power constraints*, at least not without proving that the identity noise covariance matrix minimizes the log-det expression in (3-3). It can be however regarded as an achievable rate lower bound to the downlink sum-rate capacity with a total sum power constraint (over all cell-sites).

Comparing the spectral efficiency of the three scheduling schemes, it is observed that the “opportunistic” intra-cell TDMA scheme outperforms the TC scheme in the low E_b^t/N_0 region, however the TC scheme becomes superior beyond some threshold E_b^t/N_0 . Both schemes are clearly superior to the WB scheme, and obviously also to deterministic TDMA, which produces an even lower spectral efficiency, as shown earlier in Subsection 2.4. These results demonstrate the significance of choosing an appropriate scheduling scheme in the uplink channel, when fading is present.

3.6 On The Impact of Restricted Cell-Site Cooperation

In the previous subsections, the downlink average per-cell sum-rate capacity was analyzed while employing a super joint pre-processor, that has full CSI, and processes the signals to be transmitted by *all* M system cell-sites. Consider now a sub-optimum transmission scheme, according to which joint processing of the signals of a cluster of no more than N cells can be employed. Thus, instead of a large joint super-transmitter, multiple reduced complexity transmitters are used (each with full CSI regarding its own cluster), and it is assumed that $M \gg N$ so that the number of sub-optimum processors (clusters) is large, and edge effects can be ignored. These reduced complexity transmitters shall be referred to henceforth as *restricted processing (RP)* transmitters. The rest of this subsection is devoted to the derivation of lower bounds to the downlink average per-cell sum-rate capacity with RP transmission schemes.

Proposition 3.5 *The downlink average per-cell sum-rate capacity with the N -cells RP transmission scheme, is lower bounded by the average per-cell sum-rate capacity of a circular cell-array model of N cells, as given by Propositions 3.2 and 3.3, further multiplied by a factor of $N/(N + 1)$.*

Proof: See App. D. ■

Starting from the particular case of non-fading channels, it is concluded from Proposition 3.5 that the downlink average per-cell sum-rate capacity with N -cells RP transmission is lower bounded by

$$\begin{aligned} C_{RP-nf,dl}(\bar{P}) &\geq \frac{N}{N+1} \frac{1}{N} \sum_{n=0}^{N-1} \log \left(1 + 2\bar{P} \left(1 + \cos \left(2\pi \frac{n}{N} \right) \right) \right) \\ &= \frac{1}{N+1} \sum_{n=0}^{N-1} \log \left(1 + 2\bar{P} \left(1 + \cos \left(2\pi \frac{n}{N} \right) \right) \right) . \end{aligned} \quad (3-12)$$

Examining the high-SNR regime for the above result, it is observed that the high-SNR slope (“pre-log”, “multiplexing gain”) for the lower bound satisfies

$$S_{\infty RP-nf} = \begin{cases} \frac{N}{N+1} & N \text{ odd,} \\ \frac{N-1}{N+1} & N \text{ even.} \end{cases} \quad (3-13)$$

This implies that in the absence of fading, when joint processing in the downlink is limited to no more than N cells, the loss in degrees of freedom is no more than a factor of $N/(N+1)$ when N is odd, or $(N-1)/(N+1)$ when N is even, as compared to the corresponding result when the full-CSI super joint pre-processor is employed ($S_\infty = 1$ for $M \rightarrow \infty$).

Analogously for Rayleigh fading channels, using the lower bound of Proposition 3.3, it is concluded that the downlink average per-cell sum-rate capacity with N -cells RP transmission, is lower bounded by

$$C_{RP-f,dl}(\bar{P}) \geq \frac{N}{N+1} \log(1 + \bar{P}((1-\epsilon) \log_e K + 2)) ; K \gg 1, 0 < \epsilon < 1, \quad (3-14)$$

while ignoring little orders of $\log_e K$. From Proposition 3.4 it follows immediately that the high-SNR slope for this lower bound satisfies

$$S_{\infty RP-f} = \frac{N}{N+1}. \quad (3-15)$$

It is observed that for Rayleigh fading channels, when joint processing in the downlink is limited to no more than N cells, the loss in degrees of freedom is no more than a factor of $N/(N+1)$, as compared to the corresponding full-CSI pre-processor (for which $S_\infty = 1$).

It should be emphasized at this point that the relatively low performance degradation due to restricted processing is a result of the particular system model, according to which each user only “sees” two cell-sites. Note in this respect that even when no CSI whatsoever is available, one loses no more than 1/2 of the total degrees of freedom, for example by employing inter-cell time sharing, transmitting either to odd or even cells. In this case a 2-fold diversity factor can also be obtained via two-cell-site cooperation in both uplink (as each user is received by two cell-sites), and downlink (for example by employing the Alamouti transmit diversity scheme [43]).

4 Summary and Conclusions

The impact of joint multiple cell-site processing was demonstrated in this paper through a simple analytically tractable circular multi-cell model. The model represents a practical soft handoff scenario, in which each user effectively “sees” (simultaneously) two cell-sites.

Both the uplink and downlink channels were considered and analyzed in terms of the average per-cell sum-rate capacity and spectral efficiency, and it was shown that joint multi-cell processing eliminates out-of-cell interference, which is traditionally considered to be a limiting factor in high-rate reliable communications.

When no fading is present, and for any block-circulant channel transfer matrix, the uplink and downlink channels were found, using the BC-MAC duality principle, to be equivalent in terms of the average per-cell sum-rate capacity, which approaches in the high-SNR regime the sum-capacity of *a single isolated cell*.

For the uplink channel, assuming no user cooperation, no transmitter CSI, and equal transmit powers, the presence of flat-fading was shown to be beneficial in terms of the average per-cell sum-rate capacity, when employing a WB transmission scheme, where all users transmit simultaneously and all bandwidth is available for coding. This scheme was shown to be superior to intra-cell TDMA scheduling in the presence of fading, whereas both schemes were shown to be equivalently optimum, in terms of the average per-cell sum-rate capacity, in the absence of fading. In fact, flat fading was observed to enhance performance for the WB scheme already for a small number of users per cell K . For example, in the low-SNR regime performance enhancement is observed for $K > 2$. The average per-cell sum-rate capacity was shown to be maximized in the large number of users per cell limit $K \gg 1$, where it is equal to the corresponding capacity of *a single isolated cell* with *two* receiving antennas and no fading. The WB transmission scheme thus eliminates the effect of out-of-cell interference, while exploiting the full array diversity gain of the system. The resulting sum-rate capacity exhibits a 3-dB power offset advantage in the high-SNR regime, as compared to the corresponding result in non-fading channels.

For the downlink, considering Rayleigh flat-fading channels, the downlink average per-cell sum-rate capacity was upper and lower bounded to within 1 bit/channel use, while focusing on the large number of users per cell limit ($K \gg 1$). As evident from the lower bound, with the introduction of Rayleigh fading, both the cell-array diversity gain (a factor of two in the model in concern), and a *multiuser diversity gain* of $\log_e K$ can be obtained, due to cooperation, and the available channel state information in both transmitting and receiving ends. The downlink average per-cell sum-rate capacity was shown to scale like $O(\log \log_e K)$, $K \gg 1$, in agreement with the previously reported scaling law for the single-cell multiple-antenna setting [39] [40]. Restricting joint processing to no more than N cells

was shown to reduce the number of degrees of freedom by no more than a factor of $N/(N+1)$. The uplink-downlink duality principle guarantees the same uplink multiuser diversity features provided that proper scheduling is employed. The crucial role of proper scheduling in the uplink was also demonstrated through some particular scheduling examples.

Although full information theoretic understanding of cellular systems is yet at its infancy, it is already rather clear that joint multi-cell processing is a key tool for enhancing performance in future systems, as demonstrated by the simple system model analyzed in this paper. Extensions of most of the reported results, for both the uplink and downlink channels, to a planar “two dimensional” cell-array, or to a setting in which each of the users “sees” more than just the two neighboring cell-sites, are straightforward although somewhat tedious. Extensions of the results to the case in which only partial side information is available to the joint multi-cell transmitter or receiver, are currently under investigation.

A Proof of Proposition 2.5

Following [35], consider a the slightly modified multi-cell model corresponding to a linear cell-array, as in the proof of Proposition 2.3, and let $\mathbf{G}_M \triangleq \mathbf{I}_M + \bar{P}\mathbf{H}_M\mathbf{H}_M^\dagger$. Applying Jensen’s inequality one gets

$$C_{\text{tdma-1}}(\bar{P}) = \lim_{M \rightarrow \infty} E \left\{ \frac{1}{M} \log \det \mathbf{G}_M \right\} \leq \lim_{M \rightarrow \infty} \frac{1}{M} \log E \{ \det \mathbf{G}_M \} , \quad (\text{A-1})$$

where $C_{\text{tdma-1}}$ denotes the average per-cell sum-rate capacity in the linear array model. In view of the three-diagonal matrix structure of \mathbf{G}_M (in the modified system model), its determinant may be expressed by the following difference equation

$$E\{\det \mathbf{G}_M\} = (1 + 2\bar{P})E\{\det \mathbf{G}_{M-1}\} - \bar{P}^2 E\{\det \mathbf{G}_{M-2}\} , \quad (\text{A-2})$$

with initial conditions $E\{\det \mathbf{G}_0\} = 0$, $E\{\det \mathbf{G}_1\} = 1 + 2\bar{P}$. The solution of (A-2) is given by [35]

$$E\{\det \mathbf{G}_M\} = \varphi(r^M - s^M) , \quad (\text{A-3})$$

where

$$\varphi = \frac{1 + 2\bar{P}}{\sqrt{1 + 4\bar{P}}} \quad ; \quad r = \frac{1 + 2\bar{P} + \sqrt{1 + 4\bar{P}}}{2} \quad ; \quad s = \frac{1 + 2\bar{P} - \sqrt{1 + 4\bar{P}}}{2} . \quad (\text{A-4})$$

Hence,

$$C_{\text{tdma-1}}(\bar{P}) \leq \lim_{M \rightarrow \infty} \frac{1}{M} \log E \{ \det \mathbf{G}_M \} = \log r , \quad (\text{A-5})$$

where the last equality follows from the fact that $r > s$, and $M \rightarrow \infty$. The proof is completed by noticing that $C_{\text{ul-nf}}(\bar{P}) = \log r$, and that $C_{\text{tdma-1}}(\bar{P})$ coincides with the corresponding result for the circular cell-array as discussed in the proof of Proposition 2.3.

B Proof of Proposition 3.2

The proof of Proposition 3.2 is based on three main observations. Taking $a_{m,k} = b_{m,k} = 1 \forall m, k$, for non-fading channels, it is observed from (3-8) that the transmit powers of the users in each of the cells (in the dual uplink channel) affect the entries only via their sums. The dual uplink optimization problem of (3-3), as a whole, is therefore a function of $\{\text{Tr}(\mathbf{D}_m)\}_{m=0}^{M-1}$, rather than a function of the individual powers of the users. Hence, all intra-cell schemes that retain the same values of $\{\text{Tr}(\mathbf{D}_m)\}_{m=0}^{M-1}$ yield the same overall sum-rate capacity. The rest of the proof therefore focuses on a setup in which only a single user is active in each cell ($K = 1$) transmitting with power $1/M$ (to satisfy the input covariance constraint of (3-3)).

A second useful observation is based on a result from [44]. Since the minimax optimization problem in concern is restricted to diagonal input covariance matrices satisfying $\text{Tr}(\mathbf{D}_M) \leq 1$ (a bounded convex subset of the general set of covariance matrices), and to diagonal noise covariance matrices satisfying $\bar{P}\text{Tr}(\mathbf{\Lambda}_M) \leq 1$ (a bounded convex set), the following Lemma holds (clearly one can restrict the minimax optimization problem to strictly positive definite noise covariance matrices).

Lemma B.1 ([44]) *For covariance matrices \mathbf{D}_M and $\mathbf{\Lambda}_M$ as in the minimax optimization*

problem of (3-3), the function

$$\log \left(\frac{\det (\mathbf{H}_M \mathcal{D}_M \mathbf{H}_M^\dagger + \mathbf{\Lambda}_M)}{\det (\mathbf{\Lambda}_M)} \right)$$

is convex in $\mathbf{\Lambda}_M$ and concave in \mathcal{D}_M .

Finally, the third observation is summarized in the following Lemma, which can be straightforwardly proven using basic properties of circulant matrices.

Lemma B.2 *Let \mathbf{A}_M be an $M \times M$ circulant matrix, and let $\mathbf{B}_M = \text{diag}(b_1, b_2, \dots, b_M)$ be an $M \times M$ diagonal matrix. Let $\mathbf{B}_M(m) \triangleq \text{diag}(b_{M-m+1}, \dots, b_M, b_1, \dots, b_{M-m})$ be the (diagonal) matrix obtained by performing m cyclic shifts on the diagonal entries of \mathbf{B}_M . Then*

$$\det (\mathbf{I}_M + \mathbf{A}_M \mathbf{B}_M \mathbf{A}_M^\dagger) = \det (\mathbf{I}_M + \mathbf{A}_M \mathbf{B}_M(m) \mathbf{A}_M^\dagger) \quad ; \quad \forall m = 0, 1, 2, \dots, M-1,$$

and

$$\frac{\det (\mathbf{A}_M \mathbf{A}_M^\dagger + \mathbf{B}_M)}{\det (\mathbf{B}_M)} = \frac{\det (\mathbf{A}_M \mathbf{A}_M^\dagger + \mathbf{B}_M(m))}{\det (\mathbf{B}_M(m))} \quad ; \quad \forall m = 0, 1, 2, \dots, M-1.$$

With the above observations in hand, the optimization problem is solved by deriving upper and lower bounds on the sum-rate capacity, and showing that the two bounds coincide. The upper bound is derived by choosing a particular noise covariance matrix in (3-3), equal to $\mathbf{\Lambda}_M^0 = \frac{1}{MP} \mathbf{I}_M$. In addition, let the remaining maximization over the input covariance matrix be written as (omitting the $1/M$ factor, and focusing on the total sum-rate)

$$\begin{aligned} \mathcal{R}_{\text{dl-ub}} &\triangleq \max_{\mathcal{D}_M} \log \det (\mathbf{I}_M + M \bar{P} \mathbf{H}_M \mathcal{D}_M \mathbf{H}_M^\dagger) \\ &\triangleq \max_{\mathcal{D}_M} \mathcal{R}_{\text{dl-ub}}(\mathcal{D}_M). \end{aligned} \tag{B-1}$$

Since for non fading channels the channel transfer matrix \mathbf{H}_M is a circulant matrix (restricting the discussion to $K = 1$), then in view of Lemma B.2, if \mathcal{D}_M^* satisfying $\text{Tr}(\mathcal{D}_M^*) \leq Q_U \leq 1$ is a solution to the maximization problem, the corresponding upper bound to the sum-rate capacity is unaffected by any cyclic shift of the diagonal entries

of \mathbf{D}_M^* (this can also be deduced from the circular symmetry of the system model). Let us denote by $\mathbf{D}_M^*(m)$ the matrix obtained by performing m cyclic shifts on the diagonal entries of the maximum achieving solution \mathbf{D}_M^* . Now, in view of the concavity of $\mathcal{R}_{\text{dl-ub}}(\mathbf{D}_M)$ in (B-1), as also indicated by Lemma B.1, it follows by Jensen's inequality that

$$\frac{1}{M} \sum_{m=0}^{M-1} \mathcal{R}_{\text{dl-ub}}(\mathbf{D}_M^*(m)) \leq \mathcal{R}_{\text{dl-ub}}\left(\frac{1}{M} \sum_{m=0}^{M-1} \mathbf{D}_M^*(m)\right). \quad (\text{B-2})$$

But from Lemma B.2 the left hand side (LHS) of (B-2) equals $\mathcal{R}_{\text{dl-ub}}(\mathbf{D}_M^*)$ and (B-2) becomes

$$\mathcal{R}_{\text{dl-ub}}(\mathbf{D}_M^*) \leq \mathcal{R}_{\text{dl-ub}}\left(\frac{1}{M} \sum_{m=0}^{M-1} \mathbf{D}_M^*(m)\right). \quad (\text{B-3})$$

Hence, the sum-rate capacity upper bound obtained with the “mixing” matrix of the right hand side (RHS) of (B-3), upper bounds the bound obtained with \mathbf{D}_M^* (which was initially supposed to be a solution to the maximization problem of (B-1)). Closely examining the diagonal elements of the “mixing” matrix, it is observed that

$$\left[\frac{1}{M} \sum_{m=0}^{M-1} \mathbf{D}_M^*(m)\right]_{j,j} = \frac{1}{M} \sum_{m=0}^{M-1} [\mathbf{D}_M^*(m)]_{j,j} = \frac{1}{M} \text{Tr}(\mathbf{D}_M^*) = \frac{Q_U}{M}, \quad (\text{B-4})$$

where the second equality follows from the fact that the “mixing” matrix contains all M cyclic shifts of the diagonal entries of the original matrix \mathbf{D}_M^* . It is therefore concluded that $\mathbf{D}_M = \frac{Q_U}{M} \mathbf{I}_M$, corresponding to a uniform power allocation in the dual uplink, must be a valid maximum achieving solution to (B-1). Substituting this solution into (B-1) yields

$$\frac{1}{M} \mathcal{R}_{\text{dl-ub}} = \frac{1}{M} \log \det \left(\mathbf{I}_M + Q_U \bar{P} \mathbf{H}_M \mathbf{H}_M^\dagger \right), \quad (\text{B-5})$$

which is observed to coincide with the average per-cell sum-rate capacity of the uplink channel as given by (2-15), while replacing \bar{P} with $Q_U \bar{P}$. Finally, observing that the expressions in (2-15) are increasing functions of the power \bar{P} , it is concluded that in order to solve (B-1) one must take $Q_U = 1$.

It should be noted at this point that the upper bound to the downlink sum-rate capacity with *equal per-cell power constraints*, as defined by (B-1), is in fact the (optimum) sum-rate capacity of the downlink channel with a *sum power constraint*. Hence, the above result

proves that (2-15) also gives the average downlink per-cell sum-rate capacity with a sum power constraint on the power transmitted by all of the system's cell-sites.

To obtain a lower bound (achievable rate), a particular input covariance matrix is chosen in (3-3), equal to $\mathbf{D}_M^0 = \frac{1}{M}\mathbf{I}_M$, and in a similar manner to the upper bounding procedure, the remaining minimization problem is defined as

$$\begin{aligned} \mathcal{R}_{\text{dl-lb}} &\triangleq \min_{\mathbf{\Lambda}_M} \log \frac{\det \left(\frac{1}{M} \mathbf{H}_M \mathbf{H}_M^\dagger + \mathbf{\Lambda}_M \right)}{\det (\mathbf{\Lambda}_M)} \\ &\triangleq \min_{\mathbf{\Lambda}_M} \mathcal{R}_{\text{dl-lb}}(\mathbf{\Lambda}_M) . \end{aligned} \quad (\text{B-6})$$

Observing that $\mathcal{R}_{\text{dl-lb}}(\mathbf{\Lambda}_M)$ cannot be minimized by a singular matrix, suppose $\mathbf{\Lambda}_M^*$ satisfying $\bar{P}\text{Tr}(\mathbf{\Lambda}_M^*) \leq Q_L \leq 1$ is a solution to the minimization problem. Let $\mathbf{\Lambda}_M^*(m)$ denote the matrix obtained by performing m cyclic shifts on the diagonal entries of $\mathbf{\Lambda}_M^*$. Now, due to the convexity of $\mathcal{R}_{\text{dl-lb}}(\mathbf{\Lambda}_M)$, as indicated by Lemma B.1, it follows by Jensen's inequality that

$$\frac{1}{M} \sum_{m=0}^{M-1} \mathcal{R}_{\text{dl-lb}}(\mathbf{\Lambda}_M^*(m)) \geq \mathcal{R}_{\text{dl-lb}} \left(\frac{1}{M} \sum_{m=0}^{M-1} \mathbf{\Lambda}_M^*(m) \right) . \quad (\text{B-7})$$

But invoking Lemma B.2 again, the LHS of (B-7) equals $\mathcal{R}_{\text{dl-lb}}(\mathbf{\Lambda}_M^*)$, and (B-7) becomes

$$\mathcal{R}_{\text{dl-lb}}(\mathbf{\Lambda}_M^*) \geq \mathcal{R}_{\text{dl-lb}} \left(\frac{1}{M} \sum_{m=0}^{M-1} \mathbf{\Lambda}_M^*(m) \right) . \quad (\text{B-8})$$

Hence, the bound obtained with the "mixing" noise covariance matrix of the RHS of (B-8), lower bounds the bound obtained with $\mathbf{\Lambda}_M^*$ (which was initially supposed to solve to the minimization problem). Examining the diagonal elements of the "mixing" covariance matrix it is observed that

$$\left[\frac{1}{M} \sum_{m=0}^{M-1} \mathbf{\Lambda}_M^*(m) \right]_{j,j} = \frac{1}{M} \sum_{m=0}^{M-1} [\mathbf{\Lambda}_M^*(m)]_{j,j} = \frac{1}{M} \text{Tr}(\mathbf{\Lambda}_M^*) = \frac{Q_L}{M\bar{P}} , \quad (\text{B-9})$$

where the second equality follows from the fact that the "mixing" matrix contains all M cyclic shifts of the diagonal entries of the original matrix $\mathbf{\Lambda}_M^*$. Hence, it is concluded that the noise covariance matrix $\mathbf{\Lambda}_M = \frac{Q_L}{M\bar{P}}\mathbf{I}_M$ is a valid minimum achieving solution of (B-6).

Substituting this solution into (B-6) yields

$$\frac{1}{M} \mathcal{R}_{\text{dl-lb}} = \frac{1}{M} \log \det \left(\frac{\bar{P}}{Q_L} \mathbf{H}_M \mathbf{H}_M^\dagger + \mathbf{I}_M \right), \quad (\text{B-10})$$

which also coincides with the average per-cell sum-rate capacity of the uplink channel as given by (2-15), but here while replacing \bar{P} with $Q_L \bar{P}$. Recalling that the expressions in (2-15) are increasing functions of the power \bar{P} , it is concluded that in order to solve the minimization problem of (B-6) one must take $Q_L = 1$.

Examining (B-10) and (B-5) for $Q_L = 1$ and $Q_U = 1$, reveals that both bounds coincide. Hence, in the absence of fading the average per-cell sum rate capacity of the downlink and uplink channels are equal and given by (2-15).

C Proof of Proposition 3.3

C.1 Lower Bound

Focusing on the dual uplink channel and examining (3-3), it is clear that employing any particular power control/scheduling policy that satisfies the input constraint (i.e., choosing a particular input covariance matrix \mathbf{D} in (3-3)), and minimizing over all noise covariance matrices that satisfy the noise covariance constraint, one gets a lower bound to the average per-cell sum-rate capacity (achievable rate). The same approach was taken in the proof of Proposition 3.2. Consider now the following particular ‘‘Threshold Crossing’’ (TC) policy, \mathcal{D}_M^0 , according to which, for some constant $L > 0$,

$$d_{m,k}^0 = \begin{cases} d & |a_{m,k}|^2, \left| \widehat{b_{m+1,k}} \right|^2 \geq L, \\ 0 & \text{otherwise.} \end{cases} \quad \forall m = 1, \dots, M, \quad k = 1, \dots, K \quad , \quad (\text{C-1})$$

where $d > 0$ is chosen to satisfy the transmit power (input covariance) constraint. With this policy, the probability that an arbitrary user transmits with non-zero power is given by

$$\Pr \left(|a_{m,k}|^2, \left| \widehat{b_{m+1,k}} \right|^2 \geq L \right) = e^{-2L} . \quad (\text{C-2})$$

Considering the large number of users per cell limit, the number of users in each cell transmitting with non-zero power crystalizes as $K \rightarrow \infty$ to

$$K_0 \triangleq K e^{-2L} . \quad (\text{C-3})$$

Accordingly, the equal transmit power d is set to $1/(K_0 M)$, in order to meet the power constraint of (3-3).

Incorporating the TC policy in (3-8), then as the number of user per cell K increases, the diagonal entries of $\mathbf{H}_M \mathcal{D}_M^0 \mathbf{H}_M^\dagger$ satisfy

$$\begin{aligned} \left[\mathbf{H}_M \mathcal{D}_M^0 \mathbf{H}_M^\dagger \right]_{(m,m)} &= \sum_{k=1}^K d_{m,k}^0 |a_{m,k}|^2 + \sum_{k=1}^K d_{\widehat{m-1},k}^0 |b_{m,k}|^2 \\ &= \frac{1}{MK_0} \left(\sum_{k=1}^K 1_{\{|a_{m,k}|^2, |b_{\widehat{m-1},k}|^2 \geq L\}} |a_{m,k}|^2 + 1_{\{|a_{\widehat{m-1},k}|^2, |b_{m,k}|^2 \geq L\}} |b_{m,k}|^2 \right) \\ &\xrightarrow{SLLN} \frac{1}{M} \left(E\{|\tilde{a}|^2\} + E\{|\tilde{b}|^2\} \right) = \frac{2}{M} (L+1) , \end{aligned} \quad (\text{C-4})$$

where \tilde{a} and \tilde{b} are the two i.i.d. random variables induced by constraining the fading coefficients to have magnitudes greater or equal to \sqrt{L} . For the SLLN to hold in (C-4), the constant L should be chosen so that $K_0 \rightarrow \infty$ as $K \rightarrow \infty$. In particular, let K_0 satisfy

$$K_0 \triangleq K e^{-2L} = f_0(K) = K^\epsilon \quad \Rightarrow \quad L = \frac{1-\epsilon}{2} \log_e K , \quad (\text{C-5})$$

for some constant $0 < \epsilon < 1$. In a similar manner to (C-4), it can also be shown that the off-diagonal entries of $\mathbf{H}_M \mathcal{D}_M^0 \mathbf{H}_M^\dagger$ vanish as $K \rightarrow \infty$, and it is easy to verify that the input power constraint of (3-3) holds a.s. with equality, since

$$\text{Tr}(\mathcal{D}_M^0) = \sum_{m=0}^{M-1} \sum_{k=1}^K d_{m,k}^0 = \frac{1}{MK_0} \sum_{m=0}^{M-1} \sum_{k=1}^K 1_{\{|a_{m,k}|^2, |b_{\widehat{m-1},k}|^2 \geq L\}} \xrightarrow{SLLN} \frac{1}{MK_0} \sum_{m=0}^{M-1} K_0 = 1 . \quad (\text{C-6})$$

Hence, for $K \gg 1$, there are approximately K_0 active users in each cell transmitting at power $d = 1/(MK_0)$, and the total average power per cell is $1/M$. The achievable sum-rate

(over *all* cells) in this setting, in view of (3-3), is given by

$$\begin{aligned}
R_{LB} &= E_{\mathbf{H}_M} \left\{ \min_{\mathbf{\Lambda}_M} \log \frac{\det \left(\mathbf{H}_M \mathcal{D}_M^0 \mathbf{H}_M^\dagger + \mathbf{\Lambda}_M \right)}{\det \left(\mathbf{\Lambda}_M \right)} \right\} \\
&\stackrel{\cong}{\cong}_{K \gg 1} \min_{\mathbf{\Lambda}_M} \log \frac{\det \left(\frac{2}{M}(L+1) \mathbf{I}_M + \mathbf{\Lambda}_M \right)}{\det \left(\mathbf{\Lambda}_M \right)} \\
&= \min_{\mathbf{\Lambda}_M} \sum_{m=0}^{M-1} \log \left(\frac{2(L+1)}{M\lambda_m} + 1 \right)
\end{aligned} \tag{C-7}$$

where $\{\lambda_m\} \triangleq [\mathbf{\Lambda}_M]_{m,m}$ are the (diagonal) elements of the noise covariance matrix $\mathbf{\Lambda}_M$, yet to be chosen to minimize the above sum expression, while satisfying the noise covariance constraint. Now since $\log(1 + c/x)$, for some constant $c > 0$, is convex in $x > 0$, Jensen's inequality can be employed to lower bound the achievable rate of (C-7) in the following manner

$$\begin{aligned}
R_{LB} &\geq \min_{\mathbf{\Lambda}_M} M \log \left(\frac{2(L+1)}{\sum_{m=0}^{M-1} \lambda_m} + 1 \right) \\
&\geq M \log \left(2\bar{P}(L+1) + 1 \right) .
\end{aligned} \tag{C-8}$$

The last inequality is obtained by substituting the noise covariance constraint of (3-3), $\bar{P}\text{Tr}(\mathbf{\Lambda}_M) \leq 1$ (recall that equal power constraints are imposed on each of the cell-sites in the system model in concern), and the bound is achieved by taking $\lambda_m = 1/(M\bar{P})$, $\forall m$. The inequality of (C-8) thus becomes an equality, and the achievable sum rate is given by

$$R_{LB} \stackrel{\cong}{\cong}_{K \gg 1} M \log \left(2\bar{P}(L+1) + 1 \right) . \tag{C-9}$$

Substituting (C-5) into (C-9), the achievable sum rate can be also written as

$$\begin{aligned}
R_{LB} &\stackrel{\cong}{\cong}_{K \gg 1} M \log \left(1 + 2\bar{P} \left(\frac{1-\epsilon}{2} \log_e K + 1 \right) \right) \\
&= M \log \left(1 + \bar{P} \left((1-\epsilon) \log_e K + 2 \right) \right) .
\end{aligned} \tag{C-10}$$

The lower bound in (3-10) is finally obtained by multiplying the above expression by $1/M$ to get the average per-cell achievable sum-rate.

It is interesting to note that (C-10) constitutes an upper bound for *any finite* K , as

observed from

$$\begin{aligned}
R_{LB} &= E_{\mathbf{H}_M} \left\{ \min_{\mathbf{\Lambda}} \log \frac{\det \left(\mathbf{H}_M \mathcal{D}_M \mathbf{H}_M^\dagger + \mathbf{\Lambda}_M \right)}{\det \left(\mathbf{\Lambda}_M \right)} \right\} \\
&\leq \min_{\mathbf{\Lambda}_M} \log \frac{\det \left(E \left\{ \mathbf{H}_M \mathcal{D}_M \mathbf{H}_M^\dagger \right\} + \mathbf{\Lambda}_M \right)}{\det \left(\mathbf{\Lambda}_M \right)} \\
&= \min_{\mathbf{\Lambda}_M} \log \frac{\det \left(\frac{2}{M} (L+1) \mathbf{I}_M + \mathbf{\Lambda}_M \right)}{\det \left(\mathbf{\Lambda}_M \right)}
\end{aligned} \tag{C-11}$$

where the inequality follows from a combination of Fatou's lemma and Jensen's inequality, and the last expression is equal to the one obtained for $K \gg 1$ in (C-7).

C.2 Upper Bound on the Average Per-Cell Sum-Rate Capacity

Starting from (3-3), and in an analogous manner to the lower bounding technique of Subsection C.1, choosing an arbitrary particular noise covariance matrix $\mathbf{\Lambda}_M^0$ that satisfies the noise covariance constraint, and then maximizing the log-det expression of the theorem over all input covariance matrices (power control/scheduling policies) that satisfy the input covariance constraint, produces an upper bound to the downlink sum-rate capacity. In particular, the noise covariance matrix $\mathbf{\Lambda}_M^0 = \frac{1}{M\bar{P}} \mathbf{I}_M$ satisfies the noise covariance constraint with equality. Hence, the sum-rate capacity is upper bounded by

$$MC_{dl}(\bar{P}) \leq E_{\mathbf{H}_M} \left\{ \max_{\mathcal{D}_M} \log \frac{\det \left(\mathbf{H}_M \mathcal{D}_M \mathbf{H}_M^\dagger + \mathbf{\Lambda}_M^0 \right)}{\det \left(\mathbf{\Lambda}_M^0 \right)} \right\}. \tag{C-12}$$

Employing the Hadamard inequality for semi-positive definite matrices on (C-12), we get

$$\begin{aligned}
MC_{dl}(\bar{P}) &\leq E_{\mathbf{H}_M} \left\{ \max_{\mathcal{D}_M} \log \frac{\prod_{m=0}^{M-1} \left(\left[\mathbf{H}_M \mathcal{D}_M \mathbf{H}_M^\dagger \right]_{(m,m)} + \left[\mathbf{\Lambda}_M^0 \right]_{(m,m)} \right)}{\det \left(\mathbf{\Lambda}_M^0 \right)} \right\} \\
&= E_{\mathbf{H}_M} \left\{ \max_{\mathcal{D}_M} \sum_{m=0}^{M-1} \log \left(\frac{1}{\lambda_m} \left(\sum_{k=1}^K d_{m,k} |a_{m,k}|^2 + \sum_{k=1}^K d_{\widehat{m-1},k} |b_{m,k}|^2 \right) + 1 \right) \right\} \\
&= E_{\mathbf{H}_M} \left\{ \max_{\mathcal{D}_M} \sum_{m=0}^{M-1} \log \left(M\bar{P} \left(\sum_{k=1}^K d_{m,k} |a_{m,k}|^2 + \sum_{k=1}^K d_{\widehat{m-1},k} |b_{m,k}|^2 \right) + 1 \right) \right\},
\end{aligned} \tag{C-13}$$

where the first equality is obtained by substituting the diagonal entries of $\mathbf{H}_M \mathbf{D}_M \mathbf{H}_M^\dagger$ as given in (3-8), and third equality follows from the particular choice of $\mathbf{\Lambda}_M^0$. Focusing on the limiting regime of a large number of users per cell, $K \gg 1$, and following [39], (C-13) may be further upper bounded by

$$\begin{aligned}
MC_{dl}(\bar{P}) &\leq E_{\mathbf{H}_M} \left\{ \max_{\mathcal{D}_M} \sum_{m=0}^{M-1} \log \left(M \bar{P} \left(\max_k \{|a_{m,k}|^2\} \sum_{k=1}^K d_{m,k} \right. \right. \right. \\
&\quad \left. \left. \left. + \max_k \{|b_{m,k}|^2\} \sum_{k=1}^K d_{\widehat{m-1,k}} \right) + 1 \right) \right\} \quad (\text{C-14}) \\
&\stackrel{\cong}{\cong} \max_{K \gg 1} \sum_{m=0}^{M-1} \log \left(M \bar{P} \left(f(K) \sum_{k=1}^K d_{m,k} + f(K) \sum_{k=1}^K d_{\widehat{m-1,k}} \right) + 1 \right),
\end{aligned}$$

where $f(K) \triangleq \log_e K + O(\log_e \log_e K)$. The last equality is based on a result of [39] (Example 1, App. A), according to which the maximum of K i.i.d. $\chi^2(2n)$ distributed random variables, x_{\max} , satisfies

$$\begin{aligned}
\Pr\{(n-2) \log_e \log_e K + O(\log_e \log_e \log_e K) \\
&\leq (x_{\max} - \log_e K) \leq \\
&\quad n \log_e \log_e K + O(\log_e \log_e \log_e K)\} \\
&\quad > 1 - O\left(\frac{1}{\log_e K}\right). \quad (\text{C-15})
\end{aligned}$$

Finally, applying Jensen's inequality, (C-14) reduces to

$$\begin{aligned}
MC_{dl}(\bar{P}) &\leq \max_{K \gg 1} \max_{\mathcal{D}_M} M \log \left(\bar{P} f(K) \sum_{m=0}^{M-1} \sum_{k=1}^K (d_{m,k} + d_{\widehat{m-1,k}}) + 1 \right) \\
&= \max_{\mathcal{D}_M} M \log (2 \bar{P} f(K) \text{Tr}(\mathbf{D}_M) + 1) \\
&= M \log (2 \bar{P} f(K) + 1), \quad (\text{C-16})
\end{aligned}$$

where the last equality follows from the input covariance constraint $\text{Tr}(\mathbf{D}_M) \leq 1$. Substituting $f(K)$ into (C-16) yields the following upper bound to the sum-rate capacity

(omitting little orders of $\log_e K$)

$$MC_{dl}(\bar{P}) \leq R_{UB} \underset{K \gg 1}{\cong} M \log(1 + 2\bar{P} \log_e K) , \quad (\text{C-17})$$

which completes the proof of Proposition 3.3. It is also worth noting here that the above upper bound holds also when $K \gg 1$ is kept fixed, while \bar{P} increases without bound. This comes in contrast to the corresponding $K \gg 1$ approximation in [39], where an *interference limited* suboptimum transmission strategy is considered, and therefore the derived capacity scaling laws apply only for finite SNRs.

D Proof of Proposition 3.5

To simplify the analysis, let it be assumed that no signals are transmitted to users that are located in cells indexed by integer multiples of $N + 1$ (clearly this lower bounds the downlink sum-rate capacity with the RP scheme). Ignoring the users of the $(N + 1)$ th cell, and its integer multiples, there is no interaction between different clusters, and therefore each RP transmitter can be considered separately. Note that in this case each cluster consists of $N + 1$ cell-sites (and N cells), and the cluster can be viewed as a *linear* cell-array, of the type considered in [7].

The resulting discrete time equivalent *downlink* channel model for a single RP transmitter, focusing without loss of generality on the first N cells, is given by the following equation

$$\check{\mathbf{y}}_{dl} = \check{\mathbf{H}}_N^\dagger \check{\mathbf{x}}_{dl} + \check{\mathbf{z}}_{dl} , \quad (\text{D-1})$$

where in an analogous manner to the full pre-processing scheme (3-1), $\check{\mathbf{H}}_N^\dagger$ is the $NK \times (N + 1)$ channel transfer matrix, $\check{\mathbf{x}}_{dl}$ is an $(N + 1) \times 1$ vector representing the signals transmitted by the $N + 1$ cell-sites of the cluster, for which an individual per-cell-site power constraint of \bar{P} is assumed, and the $NK \times 1$ vector $\check{\mathbf{z}}_{dl} \sim \mathcal{N}_c(\mathbf{0}, \mathbf{I}_{NK})$ denotes the vector of zero-mean circularly symmetric AWGNs at the mobile receivers. The $(N + 1) \times NK$ matrix $\check{\mathbf{H}}_N$ is a

two-block-diagonal matrix given by:

$$\check{\mathbf{H}}_N = \begin{pmatrix} \mathbf{a}_1 & \mathbf{0} & \cdots & \mathbf{0} & \mathbf{0} \\ \mathbf{b}_2 & \mathbf{a}_2 & \mathbf{0} & \cdots & \mathbf{0} \\ \mathbf{0} & \mathbf{b}_3 & \mathbf{a}_3 & \ddots & \vdots \\ \vdots & \ddots & \ddots & \ddots & \mathbf{0} \\ \mathbf{0} & \cdots & \mathbf{0} & \mathbf{b}_N & \mathbf{a}_N \\ \mathbf{0} & \cdots & \mathbf{0} & \mathbf{0} & \mathbf{b}_{N+1} \end{pmatrix}, \quad (\text{D-2})$$

where \mathbf{a}_m and \mathbf{b}_m are $1 \times K$ row vectors denoting the channel complex fading coefficients, experienced by the K users of the cells to the right and left of the m th cell-site, respectively. The fading coefficients are assumed to have exactly the same statistical properties as detailed in Section 2.

Following Yu and Lan [3], consider now the dual uplink channel given by

$$\check{\mathbf{y}}_{ul} = \check{\mathbf{H}}_N \check{\mathbf{x}}_{ul} + \check{\mathbf{z}}_{ul}, \quad (\text{D-3})$$

and let $\mathcal{D}_N \triangleq E \left\{ \check{\mathbf{x}}_{ul} \check{\mathbf{x}}_{ul}^\dagger \right\}$ denote the $NK \times NK$ diagonal input covariance matrix for this channel. Also let

$$\mathbf{\Lambda}_{N+1} \triangleq \text{diag}(\lambda_1, \dots, \lambda_{N+1}). \quad (\text{D-4})$$

denote the diagonal covariance matrix of the zero mean circularly symmetric AWGN vector $\check{\mathbf{z}}_{ul}$. In view of Theorem 3.1, the downlink sum-rate capacity for the cluster of N cells is given by:

$$C_{N,dl}(\bar{P}) = E_{\check{\mathbf{H}}_N} \left\{ \min_{\mathbf{\Lambda}_{N+1}} \max_{\mathcal{D}_N} \log \frac{\det \left(\check{\mathbf{H}}_N \mathcal{D}_N \check{\mathbf{H}}_N^\dagger + \mathbf{\Lambda}_{N+1} \right)}{\det \left(\mathbf{\Lambda}_{N+1} \right)} \right\}, \quad (\text{D-5})$$

where \mathcal{D}_N and $\mathbf{\Lambda}_{N+1}$ are subject to the trace constraints

$$\text{Tr} \mathcal{D}_N \leq 1 \quad ; \quad \text{Tr} \mathbf{\Lambda}_{N+1} \leq 1/\bar{P}. \quad (\text{D-6})$$

It is now observed that the $\log(\cdot)$ expression in (D-5) is in fact equal to the conditional input-output mutual information of the dual uplink channel (D-3), for given input and

noise covariance matrices, that is

$$I(\check{\mathbf{x}}_{ul}; \check{\mathbf{y}}_{ul} | \check{\mathbf{H}}_N) = \log \frac{\det \left(\check{\mathbf{H}}_N \mathcal{D}_N \check{\mathbf{H}}_N^\dagger + \mathbf{\Lambda}_{N+1} \right)}{\det \left(\mathbf{\Lambda}_{N+1} \right)}. \quad (\text{D-7})$$

Also, from the data processing inequality it follows that

$$\begin{aligned} I(\check{\mathbf{x}}_{ul}; \check{\mathbf{y}}_{ul} | \check{\mathbf{H}}_N) &= I([\check{\mathbf{x}}_{ul}]_1, \dots, [\check{\mathbf{x}}_{ul}]_{NK}; [\check{\mathbf{y}}_{ul}]_1, \dots, [\check{\mathbf{y}}_{ul}]_{N+1} | \check{\mathbf{H}}_N) \\ &\geq I([\check{\mathbf{x}}_{ul}]_1, \dots, [\check{\mathbf{x}}_{ul}]_{NK}; ([\check{\mathbf{y}}_{ul}]_1 + [\check{\mathbf{y}}_{ul}]_{N+1}), [\check{\mathbf{y}}_{ul}]_2, \dots, [\check{\mathbf{y}}_{ul}]_N | \check{\mathbf{H}}_N) \end{aligned}, \quad (\text{D-8})$$

where the mutual information in the last inequality may be considered as representing a modified system with N cell-sites, in which the signal received at cell-site 1 is the sum of the signals received at cell-sites 1 and $N + 1$ of the original linear cell-array. But this sum, $([\check{\mathbf{y}}_{ul}]_1 + [\check{\mathbf{y}}_{ul}]_{N+1})$, which equals

$$([\check{\mathbf{y}}_{ul}]_1 + [\check{\mathbf{y}}_{ul}]_{N+1}) = \sum_{k=1}^K a_{1,k} [\check{\mathbf{x}}_{ul}]_k + \sum_{k=1}^K b_{N+1,k} [\check{\mathbf{x}}_{ul}]_{(N-1)K+k} + [\check{\mathbf{z}}_{ul}]_1 + [\check{\mathbf{z}}_{ul}]_{N+1}, \quad (\text{D-9})$$

in fact resembles the signal that would have been received in cell-site 1, had it been assumed that the cluster's cells were ordered on a *circle*, with N cell-sites, so that the signals transmitted by the users of the N th cell in the dual uplink channel are also received at cell-site 1. The only difference is that, as can be observed from (D-9), by adding the signals received at cell-sites 1 and $N + 1$, the resulting signal includes the aggregate noise of the two cell-sites. By defining the $N \times NK$ matrix

$$\check{\mathbf{H}}_N^C = \begin{pmatrix} \mathbf{a}_1 & \mathbf{0} & \cdots & \mathbf{0} & \mathbf{b}_1 \\ \mathbf{b}_2 & \mathbf{a}_2 & \mathbf{0} & \cdots & \mathbf{0} \\ \mathbf{0} & \mathbf{b}_3 & \mathbf{a}_3 & \ddots & \vdots \\ \vdots & \ddots & \ddots & \ddots & \mathbf{0} \\ \mathbf{0} & \cdots & \mathbf{0} & \mathbf{b}_N & \mathbf{a}_N \end{pmatrix}, \quad (\text{D-10})$$

where \mathbf{b}_1 is of exactly the same distribution as \mathbf{b}_{N+1} (a mere change of notation), one can

write

$$I([\tilde{\mathbf{x}}_{ul}]_1, \dots, [\tilde{\mathbf{x}}_{ul}]_{NK}; ([\tilde{\mathbf{y}}_{ul}]_1 + [\tilde{\mathbf{y}}_{ul}]_{N+1}), [\tilde{\mathbf{y}}_{ul}]_2, \dots, [\tilde{\mathbf{y}}_{ul}]_N | \check{\mathbf{H}}_N^C) \\ = \log \frac{\det \left(\check{\mathbf{H}}_N^C \mathcal{D}_N \check{\mathbf{H}}_N^{C\dagger} + \check{\mathbf{\Lambda}}_N \right)}{\det (\check{\mathbf{\Lambda}}_N)}, \quad (\text{D-11})$$

where

$$\check{\mathbf{\Lambda}}_N \triangleq \text{diag}((\lambda_1 + \lambda_{N+1}), \lambda_2, \dots, \lambda_N), \quad (\text{D-12})$$

and $\{\lambda\}_1^{N+1}$ are the diagonal entries of $\mathbf{\Lambda}_{N+1}$ as defined in (D-4). It can therefore be concluded that

$$C_{N,dl}(\bar{P}) = E_{\check{\mathbf{H}}_N} \left\{ \min_{\{\mathbf{\Lambda}_{N+1}: \text{Tr} \mathbf{\Lambda}_{N+1} \leq \frac{1}{\bar{P}}\}} \max_{\{\mathcal{D}_N: \text{Tr} \mathcal{D}_N \leq 1\}} \log \frac{\det \left(\check{\mathbf{H}}_N^C \mathcal{D}_N \check{\mathbf{H}}_N^{C\dagger} + \mathbf{\Lambda}_{N+1} \right)}{\det (\mathbf{\Lambda}_{N+1})} \right\} \\ \stackrel{(a)}{\geq} E_{\check{\mathbf{H}}_N^C} \left\{ \min_{\{\mathbf{\Lambda}_{N+1}: \text{Tr} \mathbf{\Lambda}_{N+1} \leq \frac{1}{\bar{P}}\}} \max_{\{\mathcal{D}_N: \text{Tr} \mathcal{D}_N \leq 1\}} \log \frac{\det \left(\check{\mathbf{H}}_N^C \mathcal{D}_N \check{\mathbf{H}}_N^{C\dagger} + \check{\mathbf{\Lambda}}_N \right)}{\det (\check{\mathbf{\Lambda}}_N)} \right\} \\ \stackrel{(b)}{=} E_{\check{\mathbf{H}}_N^C} \left\{ \min_{\{\tilde{\mathbf{\Lambda}}_N: \text{Tr} \tilde{\mathbf{\Lambda}}_N \leq \frac{1}{\bar{P}}\}} \max_{\{\mathcal{D}_N: \text{Tr} \mathcal{D}_N \leq 1\}} \log \frac{\det \left(\check{\mathbf{H}}_N^C \mathcal{D}_N \check{\mathbf{H}}_N^{C\dagger} + \tilde{\mathbf{\Lambda}}_N \right)}{\det (\tilde{\mathbf{\Lambda}}_N)} \right\} \\ \triangleq C_{N,dl}^C(\bar{P}), \quad (\text{D-13})$$

where $\tilde{\mathbf{\Lambda}}_N \triangleq \text{diag}(\tilde{\lambda}_1, \dots, \tilde{\lambda}_N)$ is an $N \times N$ covariance matrix. Here (b) follows from the observation that the $\log(\cdot)$ expression in the minimax optimization at the right-hand-side of (a), depends on λ_1 and λ_{N+1} only through their sum (see (D-12)), and therefore the solution to the minimax problem will not be affected if the minimization part is restricted to sets $\{\lambda_n\}_{n=1}^{N+1}$ for which $\lambda_{N+1} = 0$, while retaining the overall trace/sum constraint (i.e., $\text{Tr} \mathbf{\Lambda}_{N+1} = \sum_{n=1}^{N+1} \lambda_n \leq 1/\bar{P}$). Hence, the minimization operation may be equivalently expressed as minimization with respect to the $N \times N$ diagonal noise covariance matrix $\tilde{\mathbf{\Lambda}}_N$, subject to $\text{Tr} \tilde{\mathbf{\Lambda}}_N = \sum_{n=1}^N \tilde{\lambda}_n \leq 1/\bar{P}$. But the resulting expression is exactly the downlink sum-rate capacity of a circular array model with N cells, as analyzed in the previous subsections, and therefore $C_{N,dl}^C(\bar{P})$ can be determined, or lower bounded, using

Propositions 3.2 and 3.3, respectively. It is hence concluded that the downlink average per-cell sum-rate capacity with the N -cell RP transmission scheme, is lower bounded by the corresponding result of Propositions 3.2 and 3.3 (while considering an N -cells circular array) multiplied by a factor of $N/(N + 1)$. The factor of $N/(N + 1)$ accounts for the fact that users of the $(N + 1)$ th cell and its multiples were ignored in the above analysis.

References

- [1] H. Dai, A. F. Molisch, and H. V. Poor, "Downlink capacity of interference-limited MIMO systems with joint detection," *IEEE Transactions on Wireless Communications*, vol. 3, pp. 442–453, Mar. 2004.
- [2] N. Laneman, D. Tse, and G. Wornell, "Cooperative diversity in wireless networks: Efficient protocols and outage behavior," *To appear in IEEE Transactions on Information Theory*, 2005. <http://www.nd.edu/~jnl/pubs/it2002.pdf>.
- [3] W. Yu and T. Lan, "Minimax duality of Gaussian vector broadcast channels," in *Proceedings of the 2004 IEEE International Symposium on Information Theory (ISIT'2004)*, (Chicago, USA), p. 177, June 27 – July 2, 2004.
- [4] N. Jindal, S. Vishwanath, and A. J. Goldsmith, "On the duality of Gaussian multiple-access and broadcast channels," *IEEE Transactions on Information Theory*, vol. 50, pp. 768–783, May 2004.
- [5] P. Viswanath and D. N. C. Tse, "Sum capacity of the vector Gaussian broadcast channel and uplink-downlink duality," *IEEE Transactions on Information Theory*, vol. 49, pp. 1912–1921, Aug. 2003.
- [6] S. Vishwanath, N. Jindal, and A. Goldsmith, "Duality, achievable rates, and sum-rate capacity of Gaussian MIMO broadcast channels," *IEEE Transactions on Information Theory*, vol. 49, no. 10, 2003.
- [7] A. D. Wyner, "Shannon-theoretic approach to a Gaussian cellular multiple-access channel," *IEEE Transactions on Information Theory*, vol. 40, pp. 1713–1727, Nov. 1994.

- [8] S. Hanly and P. Whiting, “Information-theoretic capacity of multi-receiver networks,” *Telecommunications Systems*, vol. 1, pp. 1–42, 1993.
- [9] O. Somekh and S. Shamai (Shitz), “Shannon-theoretic approach to a Gaussian cellular multi-access channel with fading,” *IEEE Transactions on Information Theory*, vol. 46, pp. 1401–1425, July 2000.
- [10] A. Grant, S. Hanly, J. Evans, and R. Müller, “Distributed decoding for Wyner cellular systems,” in *Proceedings of the 2004 Australian Communication Theory Workshop (AusCTW2004)*, (Newcastle, Australia), Feb 4–6, 2004.
- [11] E. Aktas, J. Evans, and S. Hanly, “Distributed decoding in a cellular multiple-access channel,” in *Proceedings of the 2004 IEEE International Symposium on Information Theory (ISIT2004)*, (Chicago, Illinois, USA), p. 484, June 27–July 2, 2004.
- [12] S. Shamai (Shitz) and A. D. Wyner, “Information-theoretic considerations for symmetric, cellular, multiple-access fading channels - Parts I & II,” *IEEE Transactions on Information Theory*, vol. 43, pp. 1877–1911, Nov. 1997.
- [13] S. Verdú and S. Shamai (Shitz), “Spectral efficiency of CDMA with random spreading,” *IEEE Transactions on Information Theory*, vol. 45, pp. 622–640, Mar. 1999.
- [14] S. Shamai (Shitz) and S. Verdú, “The impact of frequency-flat fading on the spectral efficiency of CDMA,” *IEEE Transactions on Information Theory*, vol. 47, pp. 1302–1327, May 2001.
- [15] A. M. Tulino and S. Verdú, “Random matrix theory and wireless communications,” *Trends in Communications and Information Theory*, vol. 1, no. 1, 2004. Now Publishers Inc. Hanover, USA.
- [16] B. M. Zaidel, S. Shamai (Shitz), and S. Verdú, “Multi-cell uplink spectral efficiency of coded DS-CDMA with random signatures,” *IEEE Journal on Selected Areas in Communications*, vol. 19, pp. 1556–1569, Aug. 2001. See also: — “Spectral Efficiency of Randomly Spread DS-CDMA in a Multi-Cell Model,” *Proceedings of the 37th Annual Allerton Conference on Communication, Control and Computing*, Monticello, IL, pp. 841–850, Sept. 1999.

- [17] B. M. Zaidel, S. Shamai (Shitz), and S. Verdú, “Multi-cell uplink spectral efficiency of randomly spread DS-CDMA in Rayleigh fading channels,” in *Proceedings of the 6th International Symposium on Communication Techniques and Applications (ISCTA '01)*, (Ambleside, UK), pp. 499–504, July 15 – 20, 2001. See also: —, “Random CDMA in the multiple cell uplink environment: the effect of fading on various receivers,” Proceedings of the 2001 IEEE Information Theory Workshop, Cairns, Australia, Sept. 2–7, 2001, pp. 42–45.
- [18] H. Dai and V. H. Poor, “Asymptotic spectral efficiency of multicell MIMO systems with frequency-flat fading,” *IEEE Transactions on Signal Processing*, vol. 51, pp. 2976–2988, Nov. 2003.
- [19] B. M. Zaidel, S. Shamai (Shitz), and S. Verdú, “Impact of out-of-cell interference on strongest-users-only CDMA detectors,” in *Proceedings of the International Symposium on Spread Spectrum Techniques and Applications (ISSSTA)*, vol. 1, (Prague, Czech Republic), pp. 258–262, Sept. 2 – 5, 2002.
- [20] S. Shamai (Shitz), B. M. Zaidel, and S. Verdú, “Strongest-users-only detectors for randomly spread CDMA,” in *Proceedings of the 2002 IEEE International Symposium on Information Theory (ISIT'2002)*, (Lausanne, Switzerland), p. 20, June 30 – July 5, 2002.
- [21] H. Li and H. V. Poor, “Power allocation and spectral efficiency of DS-CDMA systems in fading channels with fixed QoS - Part I: Single-rate case,” technical report, Princeton University, 2004.
- [22] O. Somekh, B. M. Zaidel, and S. Shamai (Shitz), “Spectral efficiency of joint multiple cell-site processors for randomly spread DS-CDMA systems,” *Submitted to the IEEE Transactions on Information Theory*, 2004. See also: —, Proc. of ISIT2004, (Chicago, USA), p. 278, June 27 – July 2, 2004.
- [23] G. Caire and S. Shamai (Shitz), “On the achievable throughput of a multi-antenna gaussian broadcast channel,” *Submitted to the IEEE Transactions on Information Theory*, 2001. See also: —, “On achievable rates in a multi-antenna broadcast downlink,” Proceedings of the 38th Annual Allerton Conference on Communication, Con-

- trol and Computing, Monticello, IL, Oct. 4–6, 2000, and the Proceedings of the 2001 IEEE International Symposium on Information Theory, Washington D.C. USA, June 24–29, 2001, p. 147.
- [24] M. H. M. Costa, “Writing on dirty paper,” *IEEE Transactions on Information Theory*, vol. IT-29, pp. 439–441, May 1983.
- [25] S. Shamai (Shitz) and B. M. Zaidel, “Enhancing the cellular downlink capacity via co-processing at the transmitting end,” in *Proceedings of the IEEE 53rd Vehicular Technology Conference (VTC 2001 Spring)*, vol. 3, (Rhodes, Greece), pp. 1745–1749, May 6–9, 2001.
- [26] S. A. Jafar and A. J. Goldsmith, “Transmitter optimization for multiple antenna cellular systems,” in *Proceedings of the 2002 IEEE International Symposium on Information Theory (ISIT’2002)*, (Lausanne, Switzerland), p. 50, June 30 – July 5, 2002.
- [27] H. Weingarten, Y. Steinberg, and S. Shamai (Shitz), “The capacity region of the Gaussian MIMO broadcast channel,” in *Proceedings of the 2004 IEEE International Symposium on Information Theory (ISIT’2004)*, (Chicago, USA), p. 174, June 27 – July 2, 2004.
- [28] A. Wiesel, Y. C. Eldar, and S. Shamai (Shitz), “Linear precoding via conic optimization for fixed mimo receivers,” *Submitted to the IEEE Transactions on Signal Processing*, 2004. See also: Proceedings of the 2004 International Zurich Seminar on Communications (IZS), ETH, Zürich, Switzerland, February, 18–20, 2004.
- [29] M. Debbah, “Capacity of a downlink MC-CDMA multi-cell network,” in *Proceedings of the IEEE International Conference on Acoustics, Speech and Signal Processing (ICASSP04)*, (Montreal, Quebec, Canada), May17–21, 2004.
- [30] S. V. H. Viswanathan and H. Huang, “Downlink capacity evaluation for cellular networks with known interference cancellation,” *IEEE Journal on Selected Areas in Communications*, vol. 21, pp. 802–811, June 2003.

- [31] S. A. Jafar, G. Foschini, and A. J. Goldsmith, “Phantomnet: Exploring optimal multi-cellular multiple antenna systems,” *EURASIP Journal on Applied Signal Processing, Special Issue on MIMO Communications and Signal Processing*, pp. 591–605, May 2004.
- [32] H. Zhang, H. Dai, and Q. Zhou, “Base station cooperation for multiuser MIMO: Joint transmission and bs selection,” in *Proceedings of the 2004 Conference on Information Sciences and Systems (CISS’2004)*, (Princeton University, Princeton, NJ), Mar. 17 – 19, 2004.
- [33] G. Foschini, H. C. Huang, K. Karakayali, R. A. Valenzuela, and S. Venkatesan, “The value of coherent base station coordination,” in *Proceedings of the 2005 Conference on Information Sciences and Systems (CISS’2005)*, (John Hopkins University, Baltimore, ML), Mar. 16 – 18, 2005.
- [34] R. M. Gray, “On the asymptotic eigenvalue distribution of Toeplitz matrices,” *IEEE Transactions on Information Theory*, vol. IT-18, pp. 725–730, Nov. 1972.
- [35] A. Narula, *Information Theoretic Analysis of Multiple-Antenna Transmission Diversity*. PhD thesis, Massachusetts Institute of Technology (MIT), Boston, MA, June 1997.
- [36] S. Verdú, “Spectral efficiency in the wideband regime,” *IEEE Transactions on Information Theory*, vol. 48, pp. 1329–1343, June 2002.
- [37] A. Lozano, A. M. Tulino, and S. Verdú, “High-SNR power offset in multi-antenna communications.” Preprint, July 2004.
- [38] W. Hirt and J. L. Massey, “Capacity of the discrete-time Gaussian channel with inter-symbol interference,” *IEEE Transactions on Information Theory*, vol. 34, pp. 380–388, May 1988.
- [39] M. Sharif and B. Hassibi, “On the capacity of MIMO broadcast channel with partial side information,” *IEEE Transactions on Information Theory*, vol. 51, pp. 506–522, Feb. 2005.

- [40] T. Yoo and A. Goldsmith, “Optimality of zero-forcing beam forming with multiuser diversity,” in *Proceedings of the IEEE International Conference on Communications (ICC 2005), Wireless Communications Theory*, (Seoul, Korea), May 16–20, 2005.
- [41] W. Yu, W. Rhee, and J. M. Cioffi, “Optimal power control in multiple access fading channels with multiple antennas,” in *Proceedings of IEEE International Conference on Communications (ICC)*, vol. 2, pp. 575–579, 2001.
- [42] W. Yu and R. W., “Degrees of freedom in multi-user spatial multiplex systems with multiple antennas,” *Submitted to IEEE Transactions on Communications*, Mar. 2004.
- [43] S. M. Alamouti, “A simple transmit diversity technique for wireless communications,” *IEEE Journal on Selected Areas in Communications*, vol. 16, pp. 1451–1458, Oct. 1998.
- [44] S. N. Diggavi and T. M. Cover, “The worst additive noise under a covariance constraint,” *IEEE Transactions on Information Theory*, vol. 47, pp. 3072–3081, Nov. 2001.

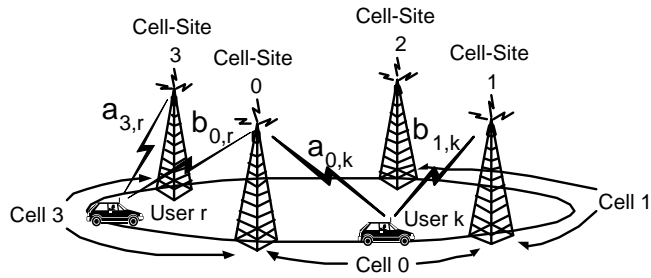


Figure 1: The circular array system model.

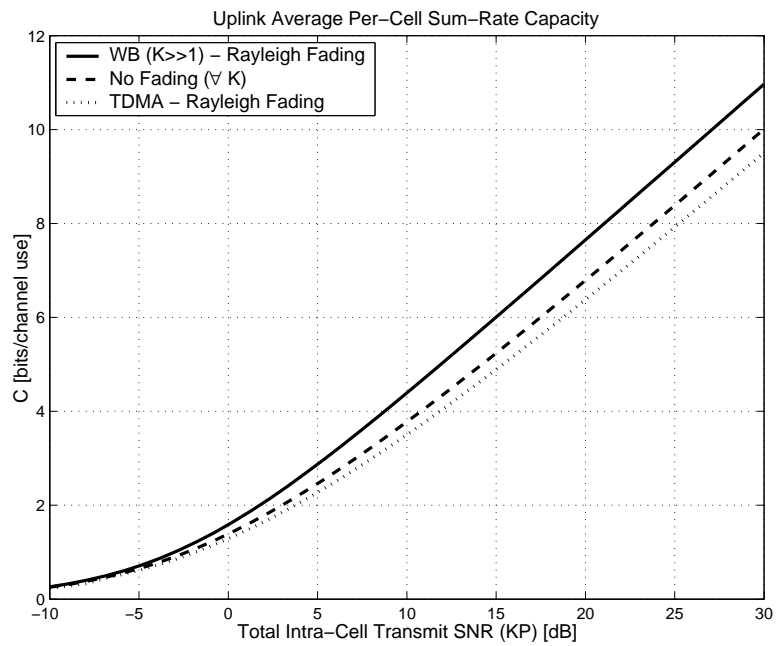


Figure 2: Uplink average per-cell sum-rate capacity.

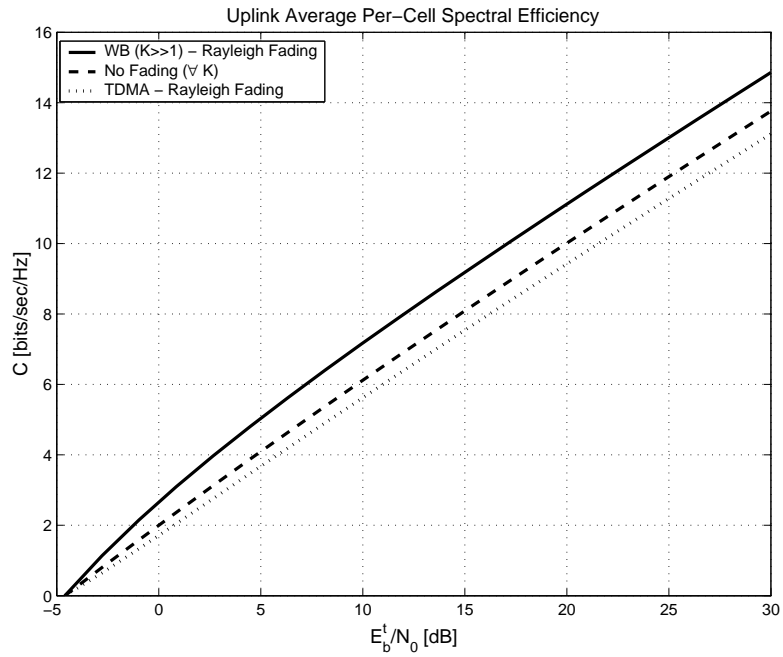


Figure 3: Uplink average per-cell spectral efficiency.

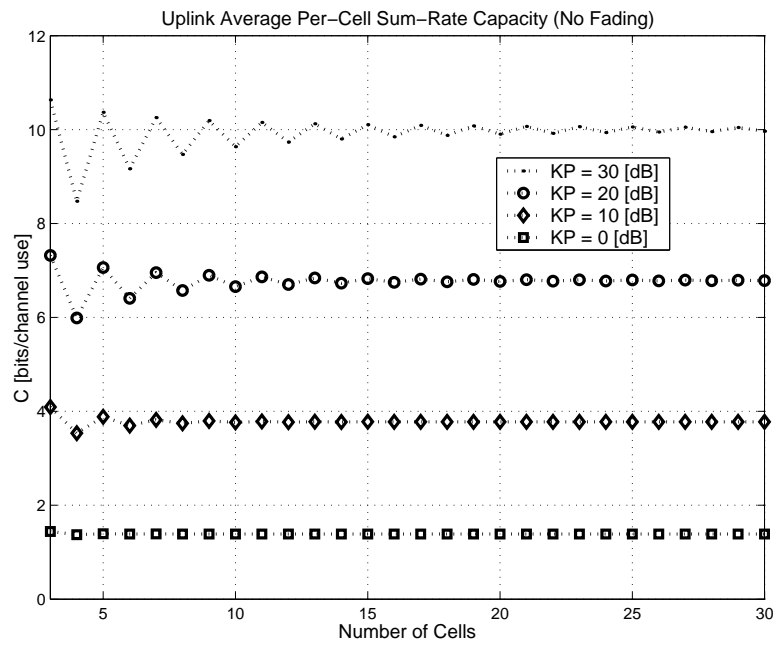


Figure 4: Uplink average per-cell sum-rate capacity vs. the number of system cells M .

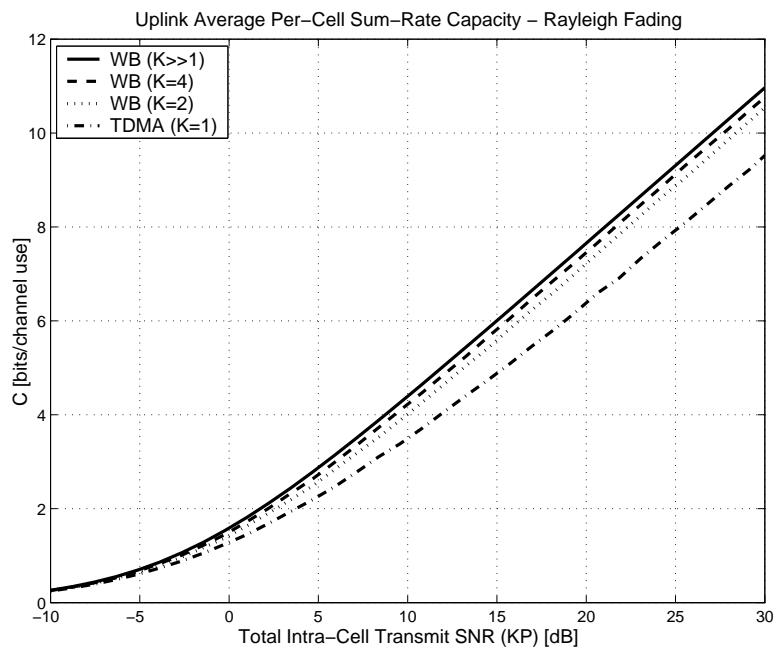


Figure 5: Uplink average per-cell sum-rate capacity for $K = 1, 2, 4, K \gg 1$ (Rayleigh fading).

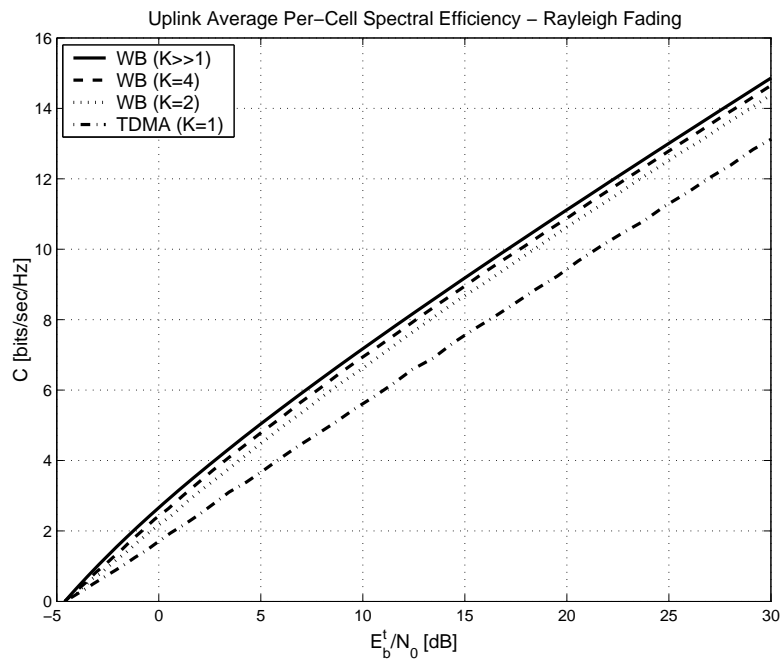


Figure 6: Uplink average per-cell spectral efficiency for for $K = 1, 2, 4, K \gg 1$ (Rayleigh fading).

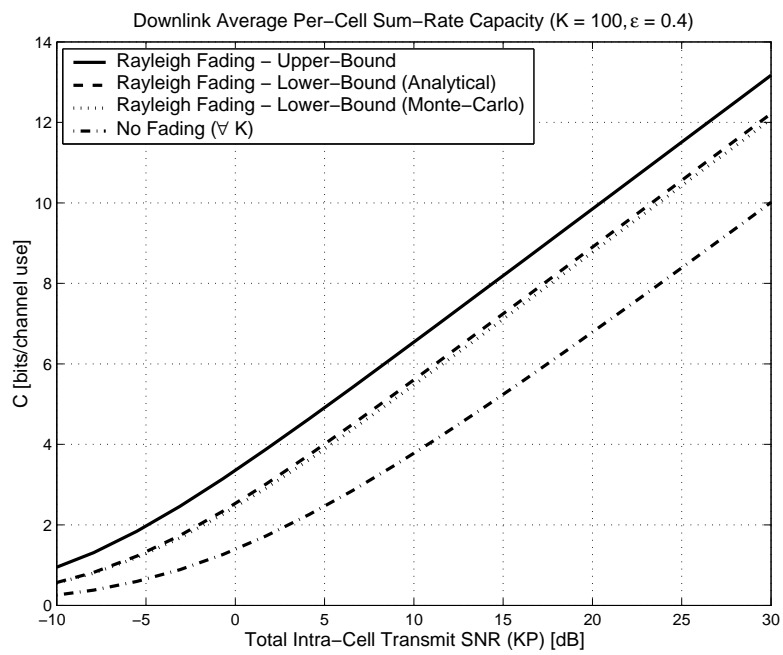


Figure 7: Downlink average per-cell sum-rate capacity, bounds evaluated for $K = 100$, $\epsilon = 0.4$.

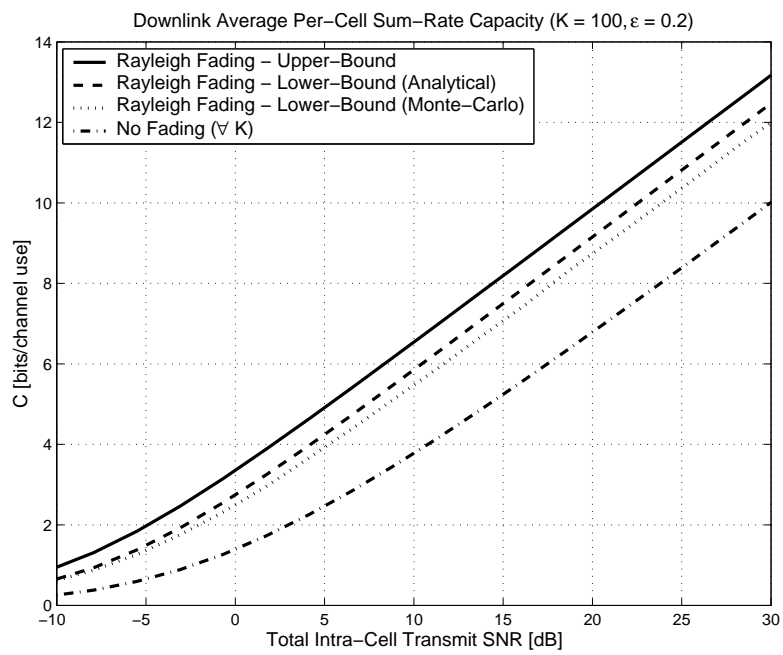


Figure 8: Downlink average per-cell sum-rate capacity, bounds evaluated for $K = 100$, $\epsilon = 0.2$.

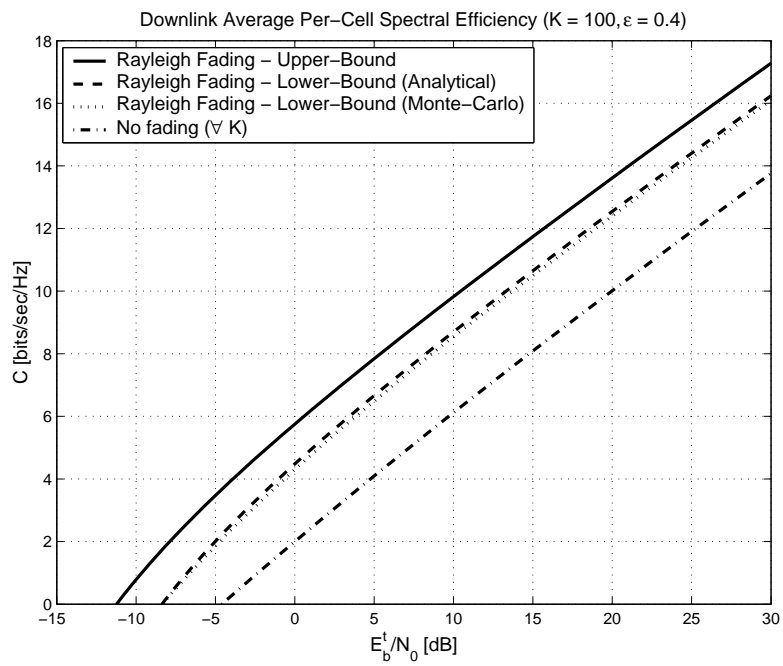


Figure 9: Downlink average per-cell spectral efficiency, bounds evaluated for $K = 100$, $\epsilon = 0.4$.

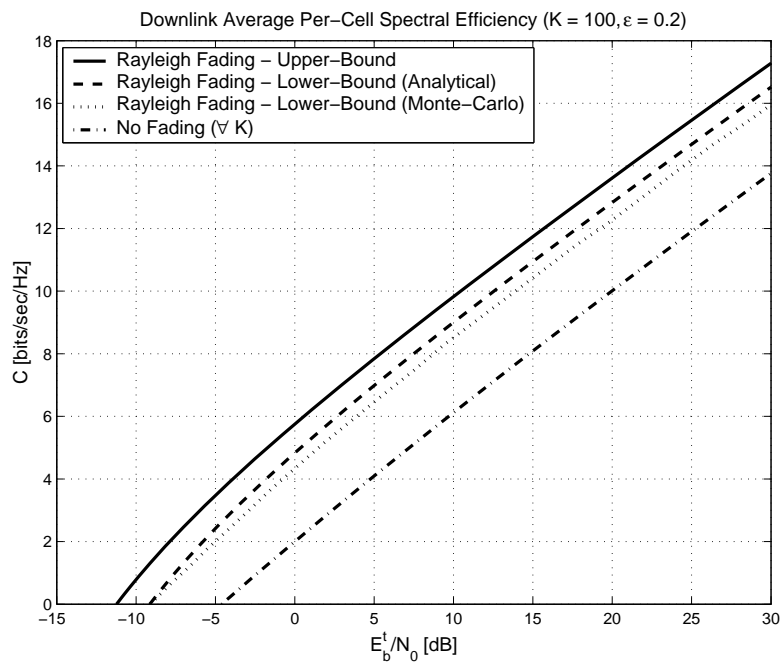


Figure 10: Downlink average per-cell spectral efficiency, bounds evaluated for $K = 100$, $\epsilon = 0.2$.

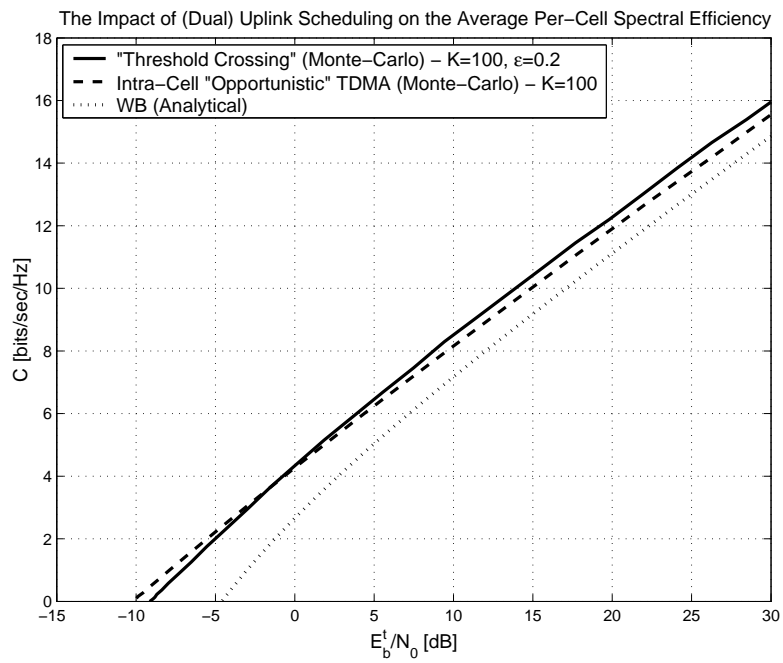


Figure 11: The impact of (dual) uplink scheduling on the average per-cell spectral efficiency ($K = 100$).